Tutorials and Reviews

International Journal of Bifurcation and Chaos, Vol. 10, No. 3 (2000) 511–548


# BIFURCATION CONTROL: THEORIES, METHODS, AND APPLICATIONS

GUANRONG CHEN*
*Department of Electrical and Computer Engineering, University of Houston, Houston, TX 77204-4793, USA*

JORGE L. MOIOLA†
*Departamento de Ingeniería Eléctrica, Universidad Nacional del Sur, Avda. Alem 1253, (8000) Bahía Blanca, Argentina*

HUA O. WANG‡
*Department of Electrical and Computer Engineering, Duke University, Durham, NC 27708-0291, USA*

Received May 10, 1999; Revised August 1, 1999

Bifurcation control deals with modification of bifurcation characteristics of a parameterized nonlinear system by a designed control input. Typical bifurcation control objectives include delaying the onset of an inherent bifurcation, stabilizing a bifurcated solution or branch, changing the parameter value of an existing bifurcation point, modifying the shape or type of a bifurcation chain, introducing a new bifurcation at a preferable parameter value, monitoring the multiplicity, amplitude, and/or frequency of some limit cycles emerging from bifurcation, optimizing the system performance near a bifurcation point, or a combination of some of these objectives. This article offers an overview of this emerging, challenging, stimulating, and yet promising field of research, putting the main subject of bifurcation control into perspective.



*Current address: Department of Electronic Engineering, City University of Hong Kong.
E-mail: gchen@uh.edu
†E-mail: comoiola@criba.edu.ar
‡E-mail: hua@ee.duke.edu

## 1. Introduction

Bifurcation control refers to the task of designing a controller to modify the bifurcation properties of a given nonlinear system, thereby achieving some desirable dynamical behaviors. Typical bifurcation control objectives include delaying the onset of an inherent bifurcation [Tesi *et al.*, 1996; Wang & Abed, 1995], introducing a new bifurcation at a preferable parameter value [Abed, 1995; Abed & Wang, 1995; Chen *et al.*, 1998b], changing the parameter value of an existing bifurcation point [Chen & Dong, 1998; Moiola & Chen, 1996], modifying the shape or type of a bifurcation chain [Wang & Abed, 1995], stabilizing a bifurcated solution or branch [Abed & Fu, 1986, 1987; Abed *et al.*, 1994; Wang & Abed, 1994, 1995; Kang, 1998a, 1998b; Laufenberg *et al.*, 1997; Littleboy & Smith, 1998; Nayfeh *et al.*, 1996; Senjyu & Uezato, 1995], monitoring the multiplicity [Calandrini *et al.*, 1999; Moiola & Chen, 1998], amplitude [Berns *et al.*, 1998a; Moiola *et al.*, 1997a], and/or frequency of some limit cycles emerging from bifurcation [Cam & Kuntman, 1998; Chen & Moiola, 1994; Chen & Dong, 1998b], optimizing the system performance near a bifurcation point [Basso *et al.*, 1998], or a combination of some of these objectives [Abed *et al.*, 1995; Chen 1998, 1999a, 1999b].

Bifurcation control with various of objectives have been implemented in experimental systems or tested by using numerical simulations in a great number of engineering, biological, and physicochemical systems; examples can be named in chemical engineering [Alhumaizi & Elnashaie, 1997; Moiola *et al.*, 1991], mechanical engineering [Liaw & Abed, 1996; Wang *et al.*, 1994b; Chen *et al.*, 1998;

Cheng, 1990; Gu *et al.*, 1997, Hackl *et al.*, 1993; Ono *et al.*, 1998; Richards *et al.*, 1997; Yabuno, 1997], electrical engineering [Chang *et al.*, 1993; Dobson & Lu, 1992; Wang *et al.*, 1994a; Goman & Khramtsovsky, 1998; Moroz *et al.*, 1992; Senjyu & Uezato, 1995; Srivastava & Srivastava, 1995; Ueta *et al.*, 1995; Volkov & Zagashvili, 1997], aeronautical engineering [Gibson *et al.*, 1998; Littleboy & Smith, 1998; Pinsky & Essary, 1994], biology [Hassard & Jiang, 1992, 1993; Invernizzi & Treu, 1991; Shiau & Hassard, 1991], physics and chemistry [Hu & Haken, 1990; Iida *et al.*, 1996; Reznik & Scholl, 1993], and metheorology [Malmgren *et al.*, 1998], to cite only a few. Bifurcation control not only is important in its own right, as further discussed in Sec. 8 below, but also suggests a viable and effective strategy for chaos control [Wang & Abed, 1994, 1995; Chen, 1999a, 1999b; Chen & Dong, 1998], because bifurcation and chaos are usually "twins" and, in particular, period-doubling bifurcation is a typical route to chaos in many nonlinear dynamical systems.

It is now known that bifurcation properties of a system can be modified via various feedback control methods. Representative approaches employ linear or nonlinear state-feedback controls [Abed & Fu, 1986, 1987; Abed *et al.*, 1994; Chen *et al.*, 1998, 1999a, 1999b; Chen *et al.*, 1998; Gu *et al.*, 1998; Kang, 1998a; Yabuno, 1997], apply a washout filter-aided dynamic feedback controller [Wang & Abed, 1995], use harmonic balance approximations [Berns *et al.*, 1998a, 1998b; Genesio *et al.*, 1993; Moiola & Chen, 1996; Tesi *et al.*, 1996] — perhaps with time-delayed feedback [Brandt & Chen, 1997; Chen *et al.*, 1999a, 1999b, 1999c; Yap & Chen, 2000], and utilize quadratic invariants in normal forms [Kang, 1998b]. This article reviews these effective methods for bifurcation control, and a few closely related topics as well as some potential real-world applications and implications to other areas of dynamical systems and controls.

Bifurcation control as an emerging research filed has become challenging, stimulating, and yet quite promising. To begin with our discussion and review, Sec. 2 first provides two typical examples to motivate this interesting and exciting research subject, and Sec. 3 briefly summarizes the ubiquitous bifurcation phenomena observed in various control systems thereby showing the importance and significance of the current study on bifurcation control. In order to describe some methodologies and to discuss some technical issues, classical bifurcation theory, for both continuous-time and discrete-time settings, are reviewed in Sec. 4. Then, a few representative techniques for controlling bifurcations, namely, the naive state-feedback method and several of its variants, as well as a few more advanced methods, are studied in Secs. 5 and 6, respectively. A closely related topic of controlling limit cycles, known also as controlling oscillations, is discussed in Sec. 7, in which the frequency domain approach is introduced. Some potential applications of bifurcation control are outlined in Sec. 8, with relevant updated references given therein. Finally, Sec. 9 concludes the article with discussions on future directions, putting the further pursuit of bifurcation control into perspectives.

## 2. Bifurcation Control — Two Examples

Before getting into the mathematical definitions of various bifurcations and the technical question of how they can be controlled, it is illuminating to discuss some control problems of two representative examples — the discrete-time Logistic map and a continuous-time model of an electric power system — to appreciate the challenge of bifurcation control. These examples illustrate some fundamental differences between bifurcation control and classical systems control, and indicate some unusual difficulties associated with this kind of control tasks.

### 2.1. *The logistic map*

The well-known Logistic map is described by

$$x_{k+1} = f(x_k, p) := px_k\,(1 - x_k)\,, \qquad (1)$$

where $p > 0$ is a real variable parameter. By solving the algebraic equation $x = f(x, p)$, two equilibria of the map can be found: $x^* = 0$ and $x^* = (p-1)/p$. Further examination of the Jacobian, $J = \partial f/\partial x = p - 2px$, reveals that the stabilities of these equilibria depend on parameter $p$.

With $0 < p < 1$, the point $x^* = 0$ is stable, and all the bounded initial points are mapped to zero as $k \to \infty$ in the system. However, it is interesting to observe that, for $1 < p < 3$, all initial points of the map converge to $x^* = (p-1)/p$ in the limit. The dynamical evolution of the system behavior, as $p$ is gradually increased from 3.0 to 4.0 by small steps, is shown in Fig. 1. This figure, which is

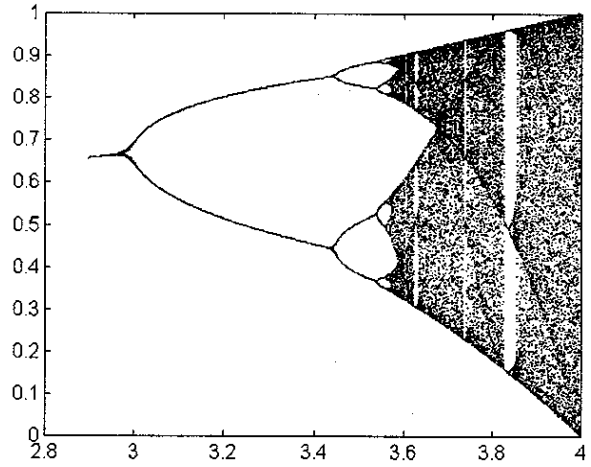


Fig. 1. Period-doubling of the Logistic system.

usually referred to as a bifurcation diagram, shows that at $p = 3$, a stable period-two orbit is born out of $x^*$, which becomes unstable at the moment, so that in addition to 0 there emerge two more stable equilibria:

$$x^{*1,*2} = (1 + p \pm \sqrt{p^2 - 2p - 3}\,)/(2p)\,.$$

When $p$ increases to the value of $1 + \sqrt{6} = 3.44948\ldots$, each of these two points bifurcates into two new points, as can be seen from the figure. These four points together constitute a period-four solution of the map (at $p = 1 + \sqrt{6}$). As $p$ moves through a sequence of values: $3.54409\ldots$, $3.5644\ldots, \ldots$, an infinite series of bifurcations is created by such *period-doubling*, which eventually leads to chaos [Argyris *et al.*, 1994]:

$$\text{period } 1 \;\rightarrow\; \text{period } 2 \;\rightarrow\; \text{period } 4 \;\rightarrow\; \cdots$$
$$\text{period } 2^{\text{k}} \;\rightarrow\; \cdots \;\rightarrow\; \text{chaos}$$

At this point, several control oriented problems may be asked: Is it possible (and, if so, how) to find a simple (say, linear) control sequence, $\{u_k\}$, to be added to the right-hand side of the Logistic map, namely,

$$x_{k+1} = f(x_k, p) = p x_k(1 - x_k) + u_k\,, \qquad (2)$$

such that, to mention just a few,

(i) the limiting chaotic behavior of the period-doubling bifurcation process is suppressed?
(ii) the first bifurcation is delayed, or this and the subsequent bifurcations are changed either in form or in stability?
(iii) the asymptotic behavior of the system becomes chaotic (if chaos is beneficial), for a parameter value of $p$ that is not in the chaotic region without control?

## 2.2. *An electric power model*

A simple yet representative electric power system is shown in Fig. 2, and is described by [Chiang *et al.*, 1990, 1994]

$$\begin{cases} \dot\theta = \omega \\ \dot\omega = 16.6667\,\sin(\theta_L - \theta + 0.0873)\,V_L - 0.1667\,\omega + 1.8807 \\ \dot\theta_L = 496.8718\,V_L^2 - 166.6667\,\cos(\theta_L - \theta - 0.0873)\,V_L \\ \qquad - 666.6667\,\cos(\theta_L - 0.2094)V_L - 93.3333\,V_L + 33.3333\,p + 43.333 \\ \dot V_L = -78.7638\,V_L^2 + 26.2172\,\cos(\theta_L - \theta - 0.0124)\,V_L \\ \qquad + 104.8689\,\cos(\theta_L - 0.1346)\,V_L + 14.5229\,V_L - 5.2288\,p - 7.0327\,, \end{cases} \qquad (3)$$

where $\theta$ is the rotational angle of the power generator, with angular velocity $\omega = \dot\theta$. In this power system, the load is represented by an induction motor, $M_I$, in parallel with a constant PQ (active-reactive) load. The variable reactive power demand, $p$, at the load bus is used as the primary system parameter. Also in the power system, the load voltage is $V_L\angle\theta_L$, with magnitude $V_L$ and angle $\theta_L$, the slack bus has terminal voltage $E\angle 0^o$ (a phasor), and the generator has terminal voltage denoted $E_m\angle\theta$.

When the system parameter $p$ is gradually increased or decreased, two sequences of complex dynamical phenomena can be observed [Abed *et al.*, 1993; Chiang *et al.*, 1990; Lee & Ajjarapu, 1993].

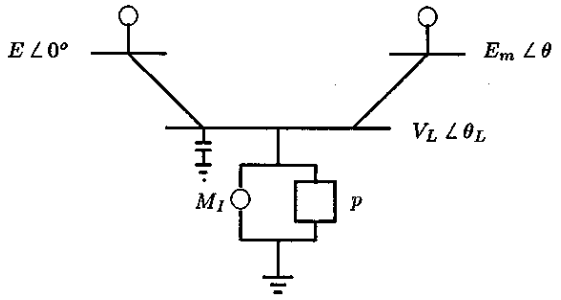


Fig. 2. A simple electric power system.

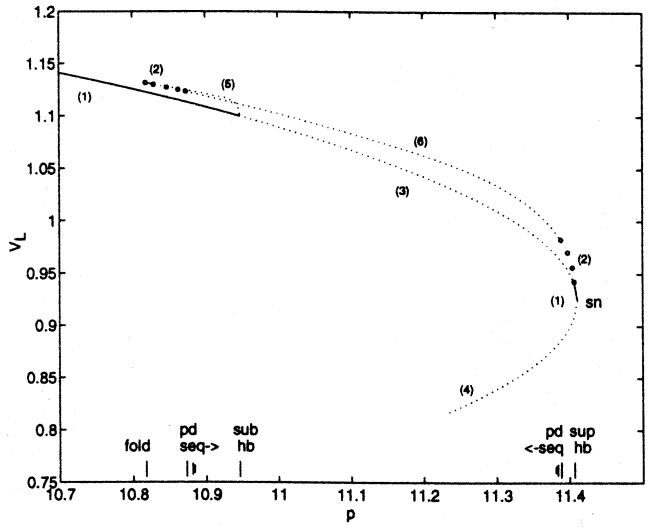


Fig. 3. Dynamics of the power network.

These are shown in Fig. 3, where on the left-hand side:

- $p = 10.818$, a turning point of periodic orbit occurs;
- $p = 10.873$, first period-doubling bifurcation occurs;
- $p = 10.882$, second period-doubling bifurcation occurs;
- $p = 10.946$, a subcritical Hopf bifurcation occurs;

on the right-hand side:

- $p = 11.410$, a saddle-node bifurcation occurs;
- $p = 11.407$, a supercritical Hopf bifurcation occurs;
- $p = 11.389$, first period-doubling bifurcation occurs;
- $p = 10.384$, second period-doubling bifurcation occurs.

In this figure, (1) denotes stable equilibria, (2) stable limit cycles, (3) and (4) different types of unstable equilibria, and (5) and (6) different types of unstable limit cycles.

The dynamics of this system with varying a second parameter (machine damping) has been studied in [Chiang *et al.*, 1994; Tan *et al.*, 1995], showing the connection of the two Hopf bifurcation points with a degenerate Hopf bifurcation and the disappearance of the chaotic behavior.

Similar to the Logistic map discussed above, a few interesting control problems are:

(i) can the limiting chaotic behavior of the period-doubling bifurcation process be suppressed?
(ii) can the first bifurcation be delayed in occurrence, or this and the subsequent bifurcations be changed either in form or in stability?
(iii) can the voltage collapse be avoided or delayed through bifurcation or chaos control?

Nonconventional control problems like these pose a real challenge to both nonlinear dynamics analysts and control engineers.

## 3. Bifurcations in Control Systems

The two examples of bifurcations in systems discussed above are simple but illustrative. In fact, various bifurcations can occur in nonlinear dynamical systems, including in systems under feedback and/or adaptive controls. This is perhaps counter-intuitive, but generally speaking, local instability and complex dynamical behavior can result from such controlled systems — if adequate process information is not available for feedback or parameter estimation. In these situations, one or more poles of the closed-loop transfer function of the linearized system may move to cross over the stability boundary, potentially leading to signal divergence as the control process continues. This, sometimes, may not lead to a global unboundedness in a complex nonlinear system, but rather, to self-excited oscillations or bifurcations [Chang *et al.*, 1993; Cui *et al.*, 1997; Golden & Ydstie, 1988, 1992; Mareels & Bitmead, 1986, 1988; Praly & Pomet, 1987; Ydstie & Golden, 1986, 1987, 1988].

Bifurcations exist in many feedback control systems, for example, in automatic gain control (AGC) loops. AGCs are very popular in industrial applications (e.g. in most receivers of communication systems). A typical structure of the AGC is shown

in Fig. 4. It is usually used to maintain a constant output level, $v_0$, of a system, with respect to a reference (bias), $v_b$, obtained from the received input signal $v_i$ via a variable gain amplifier (VGA) and a control signal, $v_c$, through a filter, $F(s)$. Here, both the VGA and the detector are nonlinear. Such an AGC loop can have homoclinic bifurcation leading to chaos [Chang *et al.*, 1993]. Its discrete version also has the common route of period-doubling bifurcations to chaos, similar to the Logistic map discussed above.

A single pendulum, controlled by a linear proportional-derivative (PD) controller, is another simple example of a feedback control system that has various bifurcations [Kelly, 1996]. Even a feedback system with a linear plant and a linear controller can produce bifurcations and chaos if a simple nonlinearity (e.g. saturation) exists in the loop [Alvarez & Curiel, 1997].

Adaptive control systems are more likely to produce bifurcations due to the changes of stabilities. Different pathways, that lead to estimator instability in a model-referenced adaptive control system, can be identified [Golden & Ydstie, 1992]. Similarly, in discrete-time adaptive control systems, rich bifurcation phenomena have been observed [Ydstie & Golden, 1987].

Bifurcations, ubiquitous in physical systems, need not subject to control. For instance, power systems generally have rich bifurcation phenomena [Chiang *et al.*, 1994; Wang *et al.*, 1994a; Hill, 1995; Ji & Venkatasubramanian, 1995; Lee & Ajjarapu, 1993; Venkatasubramanian & Ji, 1999]. In particular, when the consumer demand for power reaches its peaks, the dynamics of an electric power network may move to its stability margin, leading to oscillations and bifurcations. This may quickly result in voltage collapse [Dobson *et al.*, 1992; Wang *et al.*, 1994a].

A typical double pendulum can display bifurcation as well as chaotic motions [Thomsen, 1995; Ueta *et al.*, 1995; Zhou & Whiteman, 1996]. Some rotational mechanical systems also have similar behaviors [Cheng, 1990]. A road vehicle under steering control can have Hopf bifurcation when it loses stability, which may also develop chaos and even hyperchaos [Liu *et al.*, 1996]. A hopping robot, even a simple two-degree-of-freedom flexible robot arm, can produce unusual vibrations and undergo period-doubling which leads to chaos [Streit *et al.*, 1988; Vakakis *et al.*, 1991]. An aircraft stalls during flight, either below a critical speed or over a critical angle-

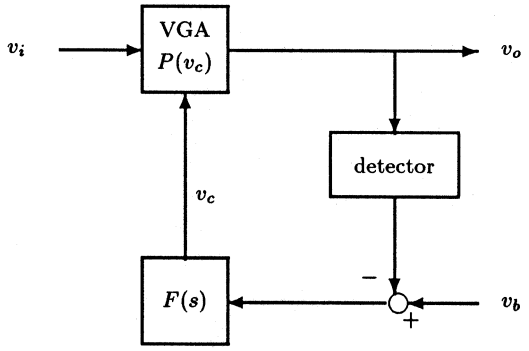


Fig. 4. Block diagram of an automatic gain control loop.

of-attack, and can respond to various bifurcations [Chapman *et al.*, 1992; Goman & Khramtsovsky, 1998]. Dynamics of ships can exhibit bifurcations according to wave frequencies that are close to the natural frequency of the ship, creating oscillations and chaotic motions leading to ship capsize [Liaw & Bishop, 1995; Sanchez & Nayfeh, 1979]. Simple nonlinear circuits are rich sources of bifurcation phenomena [Chan & Tse, 1996; Madan, 1993; Matsumoto, 1987; Tse, 1994]. Many other systems have bifurcation properties, including cellular neural networks [Chua, 1998; Zou & Nossek, 1993], laser, aeroengine compressors, weather, and biological population dynamics [Abed *et al.*, 1995].

Therefore, controlling bifurcations indeed will have a tremendous impact on real-world applications and its significance in both dynamics analysis and systems control will be enormous, profound, and far-reaching.

## 4. Bifurcation Preliminaries

Before control methods can be discussed, mathematical definitions of various bifurcations are introduced in this section.

For this purpose, it is convenient to consider a two-dimensional, parametrized, nonlinear dynamical system,

$$\begin{cases} \dot{x} = f(x, y; p) \\ \dot{y} = g(x, y; p)\,, \end{cases} \tag{4}$$

where $p$ is a real variable system parameter.

Let $(x^*, y^*) = (x^*(p_0), y^*(p_0))$ be an equilibrium point of the system at $p = p_0$, satisfying $f(x^*, y^*; p_0) = 0$ and $g(x^*, y^*; p_0) = 0$. If the equilibrium point is stable (resp. unstable) for $p > p_0$ but unstable (resp. stable) for $p < p_0$, then $p_0$ is a *bifurcation value* of $p$, and $(0, 0, p_0)$ is a *bifurca-*

*tion point* in the *parameter space* of coordinates $x$-$y$-$p$. A few examples are given below to distinguish several different but typical bifurcations.

### 4.1. *Bifurcations of one-dimensional maps*

The one-dimensional system

$$\dot{x} = f(x; p) = px - x^2$$

has two equilibria: $x_1^* = 0$ and $x_2^* = p$. If $p$ is varied, then there are two equilibrium curves (see Fig. 5, where the $t$-axis is the variable of $x = x(t)$ which may help better visualization of the dynamics). Since the Jacobian of the system is $J = \partial f/\partial x|_{x=0} = p$, it is clear that for $p < p_0 = 0$, the equilibrium $x_1^* = 0$ is stable, but for $p > p_0 = 0$ it becomes unstable. Hence, $(x_1^*, p_0) = (0, 0)$ is a bifurcation point. In this and the following figures, the solid curves indicate stable equilibria and the dashed curves, the unstable ones. Similarly, one can verify that $(x_2^*, p_0)$ is another bifurcation point. This is called a *transcritical bifurcation.*

The one-dimensional system

$$\dot{x} = f(x; p) = p - x^2$$

has an equilibrium point, $x_1^* = 0$, at $p_0 = 0$, and an equilibrium curve, $(x^*)^2 = p$, at $p \geq 0$, where $x_2^* = \sqrt{p}$ is stable and $x_3^* = -\sqrt{p}$ is unstable for $p > p_0 = 0$. This is called a *saddle-node bifurcation* (see Fig. 6).

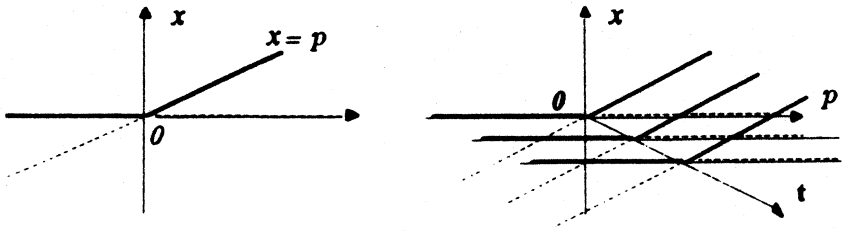


Fig. 5. The transcritical bifurcation.

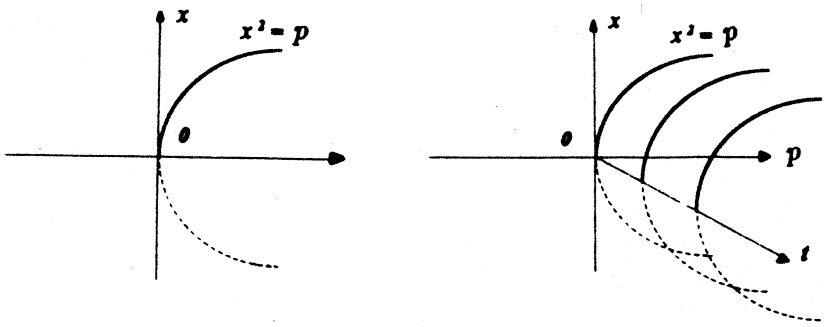


Fig. 6. The saddle-node bifurcation.

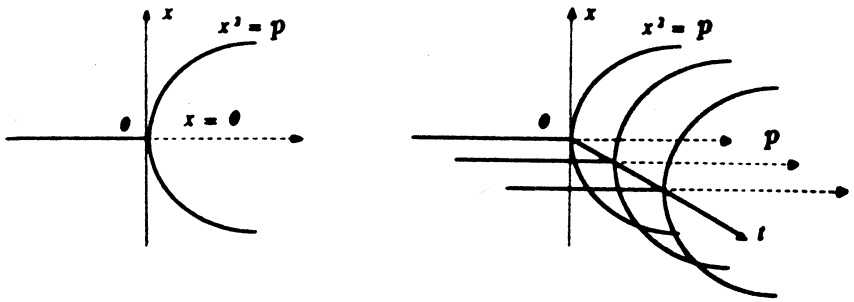


Fig. 7. The pitchfork bifurcation.

The one-dimensional system

$$\dot{x} = f(x;\, p) = px - x^3$$

has an equilibrium point, $x_1^* = 0$, at $p_0 = 0$, and an equilibrium curve, $(x^*)^2 = p$, at $p \geq 0$. Its Jacobian is $J = p - 3(x^*)^2$, so $x_1^* = 0$ is unstable for $p > p_0 = 0$ and stable for $p < p_0 = 0$. Also, the entire equilibrium curve $(x^*)^2 = p$ is stable for all $p > 0$ (at which the Jacobian is $J = -2p$). This is called a *pitchfork bifurcation*, and is depicted in Fig. 7.

An equivalent analysis for these elementary static bifurcations using a frequency domain approach is also possible [Moiola *et al.*, 1997b].

Note, however, that not all nonlinear dynamical systems have bifurcations. This can be easily verified by similarly analyzing the following example:

$$\dot{x} = f(x;\, p) = p - x^3\,.$$

This equation has an entire stable equilibrium curve, $x = p^{1/3}$, and, thus, does not have any bifurcations.

### 4.2. *Hopf bifurcation of higher-dimensional systems*

The bifurcation phenomena discussed above for one-dimensional parametrized nonlinear maps are

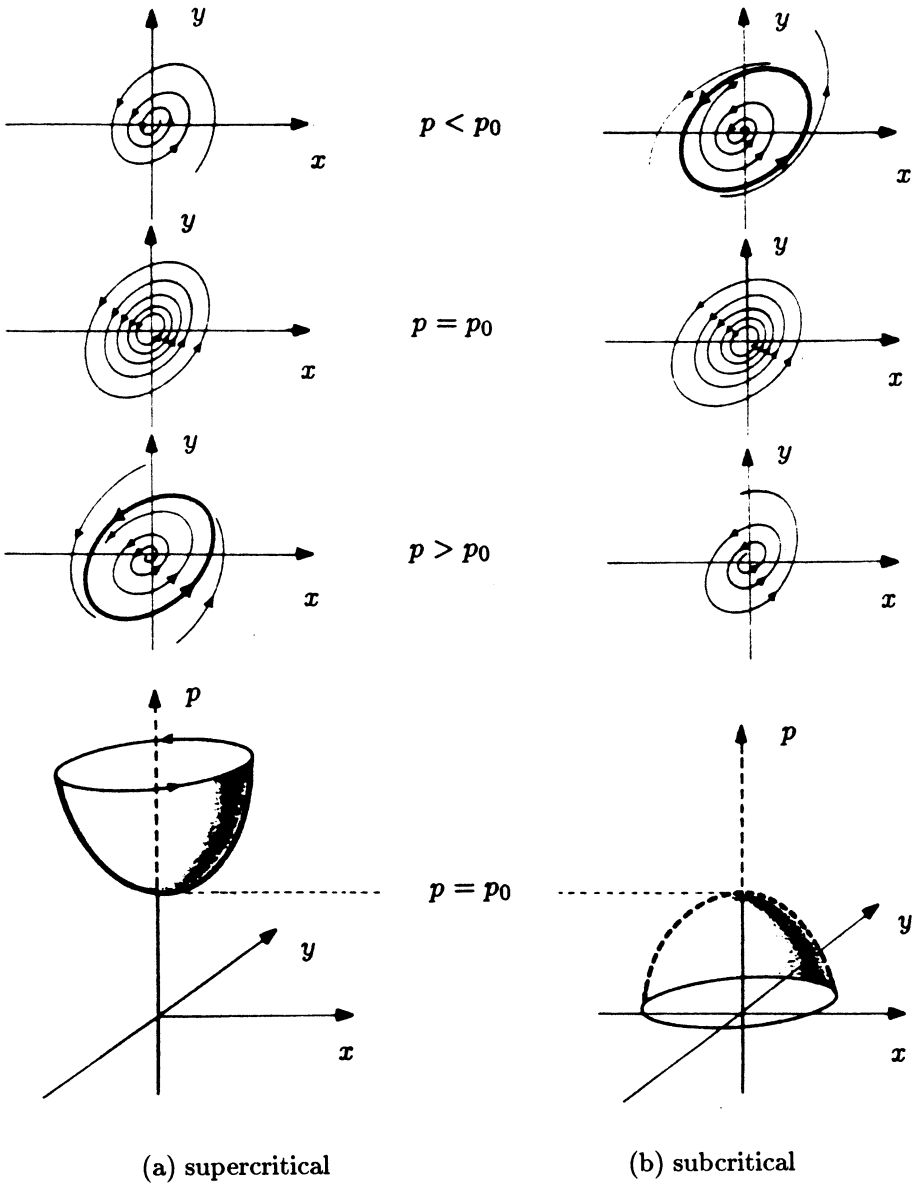


Fig. 8. Two types of Hopf bifurcation in the phase plane.

usually referred to as *static bifurcations*. In higher-dimensional systems or maps, the situation is more complicated. For instance, there is an additional bifurcation phenomenon for systems of dimension two or higher — the *Hopf bifurcation*, referred to as a *dynamic bifurcation*.

A Hopf bifurcation corresponds to the situation where, as the parameter $p$ is varied to pass a critical value $p_0$, the system Jacobian has one pair of complex conjugate eigenvalues moving from the left-half plane to the right, crossing the imaginary axis, while all the other eigenvalues remain stable. At that moment of crossing, the real parts of the two eigenvalues become zero, and the stability of the existing equilibrium changes from being stable to unstable. Also, at the moment of crossing, a limit cycle is born. These phenomena are supported by the following classical result [Arrowsmith & Place, 1990] (see Fig. 8):

**Theorem** (Poincaré–Andronov–Hopf). *Suppose that the two-dimensional system (4) has a zero equilibrium,* $(x^*, y^*) = (0, 0)$, *and that its associate Jacobian has a pair of purely imaginary eigenvalues,* $\lambda(p)$ *and* $\bar{\lambda}(p)$. *If*

$$\left.\frac{d\Re\{\lambda(p)\}}{dp}\right|_{p=p_0} > 0$$

*for some* $p_0$, *then*

(i) $p = p_0$ *is a bifurcation point of the system*;
(ii) *for close enough values* $p < p_0$, *the zero equilibrium is asymptotically stable*;
(iii) *for close enough values* $p > p_0$, *the zero equilibrium is unstable*;
(iv) *for close enough values* $p \neq p_0$, *the zero equilibrium is surrounded by a limit cycle of magnitude* $O(\sqrt{|p - p_0|})$.

As indicated in Fig. 8, the Hopf bifurcations are classified as *supercritical* (resp. *subcritical*) if the equilibrium is changed from stable to unstable (resp. from unstable to stable). In other words, the periodic solutions have opposite stabilities as the equilibria. Note that the same terminology of supercritical and subcritical bifurcations apply to other non-Hopf types of bifurcations.

For the discrete-time setting, consider a two-dimensional parametrized system:

$$\begin{cases} x_{k+1} = f(x_k, y_k; p) \\ y_{k+1} = g(x_k, y_k; p)\,, \end{cases} \tag{5}$$

with a real variable parameter $p \in R$ and an equilibrium point $(x^*, y^*)$, satisfying $x^* = f(x^*, y^*; p)$ and $y^* = g(x^*, y^*; p)$ simultaneously for all $p$ in a neighborhood of $p^* \in R$. Let $J(p)$ be its Jacobian at this equilibrium, and $\lambda_{1,2}(p)$ be its eigenvalues, with $\lambda_2(p) = \bar{\lambda}_1(p)$. If

$$|\lambda_1(p^*)| = 1 \quad \text{and} \quad \left.\frac{\partial|\lambda_1(p)|}{\partial p}\right|_{p=p^*} > 0 \tag{6}$$

the system undergoes a *Hopf bifurcation* at $(x^*, y^*, p^*)$, in a way analogous to the continuous-time setting. Both supercritical and subcritical Hopf bifurcations can be distinguished for the discrete case, via a sequence of coordinate transformations [Glendinning, 1994; Hale & Koçak, 1991].

## 5. Basic State Feedback Bifurcation Control Methods

To introduce some basic and direct state feedback control methods, consider a one-dimensional, discrete-time, parametrized, nonlinear control system of the form

$$x_{k+1} = F(x_k; p) := f(x_k; p) + u(x_k; p)\,, \tag{7}$$

where $p \in R$ is a variable parameter, $x_0 \in R$ is the initial state, and $u(\cdot)$ is the state feedback controller to be designed. The map $F$: $R \to R$ is autonomous under this framework, which represents the dynamical behaviors of the control system visualized in the $x_k$-$x_{k+1}$ phase plane, $k = 0, 1, 2, \ldots$.

The bifurcation analysis for this control system is formulated as the following routine step-by-step checking procedure for convenience in the design of the controller.

### 5.1. *Controlling saddle-node, transcritical, and pitchfork bifurcations*

The first procedure is used for determining the transcritical, pitchfork, and saddle-node types of bifurcations, as well as the stabilities of the equilibria. The period-doubling bifurcation is discussed in the next subsection.

***Step 0.*** Initiate a structure of the controller (e.g. a linear state feedback controller) in system (7).

***Step 1.*** Solve the equilibrium equation

$$x^* = F(x^*; p)\,, \quad p \in R\,, \tag{8}$$

for a solution $x^*(t; p)$; if no solution, change the structure of the controller and try again.

***Step 2.*** Determine the bifurcating parameter value, $p = p^*$, such that

$$\left.\frac{\partial F}{\partial x}\right|_{\substack{x=x^*\\p=p^*}} = 1\,; \tag{9}$$

if no solution, change the structure of the controller, and then return to Step 1.

***Step 3.*** Determine the type of the bifurcation according to the classification given in Table 1.

Table 1. Classification of three typical types of bifurcations.

| $\left.\frac{\partial F}{\partial p}\right\|_{\substack{x=x^*\\p=p^*}}$ | $\left.\frac{\partial^2 F}{\partial x^2}\right\|_{\substack{x=x^*\\p=p^*}}$ | Bifurcations |
|---|---|---|
| $\neq 0$ | $\neq 0$ | saddle-node |
| $= 0$ | $\neq 0$ | transcritical |
| $= 0$ | $= 0$ | pitchfork |

***Step 4.*** Determine the stability of the equilibria according to Tables 2–4.

Table 2. Stability of equilibria near a saddle-node bifurcation.

| $\left.\frac{\partial F}{\partial p}\right\|_{\substack{x=x^*\\p=p^*}}$ | $\left.\frac{\partial^2 F}{\partial x^2}\right\|_{\substack{x=x^*\\p=p^*}}$ | Stable Equilibrium | Unstable Equilibrium | No Equilibrium |
|---|---|---|---|---|
| $> 0$ | $> 0$ | $p < p^*$ (upper) | $p < p^*$ (lower) | $p > p^*$ |
| $> 0$ | $< 0$ | $p > p^*$ (upper) | $p > p^*$ (lower) | $p < p^*$ |
| $< 0$ | $> 0$ | $p > p^*$ (lower) | $p > p^*$ (upper) | $p < p^*$ |
| $< 0$ | $< 0$ | $p < p^*$ (lower) | $p < p^*$ (upper) | $p > p^*$ |

Table 3. Stability of equilibria near a transcritical bifurcation.

| $\left.\frac{\partial^2 F}{\partial x \partial p}\right\|_{\substack{x=x^*\\p=p^*}} - \left.\frac{\partial^2 F}{\partial x^2}\frac{\partial^2 F}{\partial p^2}\right\|_{\substack{x=x^*\\p=p^*}}$ | $\left.\frac{\partial^2 F}{\partial x^2}\right\|_{\substack{x=x^*\\p=p^*}}$ | Stable Equilibrium | Unstable Equilibrium |
|---|---|---|---|
| $\neq 0$ | $> 0$ | (lower) | (upper) |
| $\neq 0$ | $< 0$ | (upper) | (lower) |

Table 4. Stability of equilibria near a pitchfork bifurcation.

| $\left.\frac{\partial^2 F}{\partial x \partial p}\right\|_{\substack{x=x^*\\p=p^*}}$ | $\left.\frac{\partial^3 F}{\partial x^3}\right\|_{\substack{x=x^*\\p=p^*}}$ | Stable Equilibrium (1st branch) | Unstable Equilibrium (1st branch) | Stable Equilibrium (2nd branch) | Unstable Equilibrium (2nd branch) |
|---|---|---|---|---|---|
| $> 0$ | $> 0$ | $p < p^*$ | $p > p^*$ | — | $p < p^*$ |
| $> 0$ | $< 0$ | $p < p^*$ | $p > p^*$ | $p > p^*$ | — |
| $< 0$ | $> 0$ | $p > p^*$ | $p < p^*$ | — | $p > p^*$ |
| $< 0$ | $< 0$ | $p > p^*$ | $p < p^*$ | $p < p^*$ | — |

## 5.2. *The period-doubling bifurcation and its control*

The following procedure can be used for determining the period-doubling bifurcation.

***Step 0.*** Initiate a structure of the controller in system (7).

***Step 1.*** Solve the equilibrium equation

$$x^* = F(x^*; p), \quad p \in R\,, \tag{10}$$

for a solution $x^*(t; p)$; if no solution, change the structure of the controller and try again.

Table 5. Stability of equilibria near a period-doubling bifurcation.

| $\xi$ | $\eta$ | Period-Doubling | Stable Equilibrium | Unstable Equilibrium |
|---|---|---|---|---|
| $> 0$ | $> 0$ | $p < p^*$ (stable) | $p > p^*$ | $p < p^*$ |
| $> 0$ | $< 0$ | $p > p^*$ (unstable) | $p > p^*$ | $p < p^*$ |
| $< 0$ | $> 0$ | $p > p^*$ (stable) | $p < p^*$ | $p > p^*$ |
| $< 0$ | $< 0$ | $p < p^*$ (unstable) | $p < p^*$ | $p > p^*$ |

***Step 2.*** Determine the bifurcating parameter value, $p = p^*$, such that

$$\left.\frac{\partial F}{\partial x}\right|_{\substack{x=x^*\\p=p^*}} = -1\,; \tag{11}$$

if no solution, change the structure of the controller, and then return to Step 1.

***Step 3.*** Determine the existence of the period-doubling bifurcation as well as the stability of the equilibria according to the classification given in Table 5, where

$$\xi = \left(2\frac{\partial^2 F}{\partial x \partial p} + \frac{\partial F}{\partial p}\frac{\partial^2 F}{\partial x^2}\right)\Bigg|_{\substack{x=x^*\\p=p^*}} \tag{12}$$

and

$$\eta = \left(\frac{1}{2}\left(\frac{\partial^2 F}{\partial x^2}\right)^2 + \frac{1}{3}\frac{\partial^3 F^2}{\partial x^3}\right)\Bigg|_{\substack{x=x^*\\p=p^*}}\,. \tag{13}$$

Therefore, by following the above procedures, a controller can be designed by satisfying the conditions listed in the corresponding tables, for controlling various bifurcations.

As an example, consider the Logistic map (1). The control objective is to shift the original bifurcation point $(x^*, p^*)$ to a new position, $(x^o, p^o)$. For this purpose, the structure of the controller can be determined as follows: First, from condition (8), one has

$$F(x^o, p^o) = p^o x^o(1 - x^o) + u\,|_{x=x^o, p=p^o} = x^o\,,$$

which gives

$$u\,|_{x=x^o, p=p^o} = x^o - p^o x^o + p^o (x^o)^2\,;$$

then from condition (9), one has

$$\left.\frac{\partial F}{\partial x}\right|_{\substack{x=x^o\\p=p^o}} = p^o - 2p^o x^o + \frac{\partial u}{\partial x}\,|_{x=x^o, p=p^o} = 1\,,$$

which yields

$$\left.\frac{\partial u}{\partial x}\right|_{\substack{x=x^o\\p=p^o}} = 1 - p^o + 2p^o x^o\,.$$

These two results together lead to

$$\begin{aligned} u(x_k;\, p) \;&=\; (1 - p^o + 2p^o x^o)x_k - p^o (x^o)^2 \\ &:= c_1 x_k + c_2\,, \end{aligned} \tag{14}$$

where $c_1 = c_1(x^o, p^o)$ and $c_2 = c_2(x^o, p^o)$.

For the controlled logistic map,

$$x_{k+1} = F(x_k;\, p) = px_k(1 - x_k) + (c_1\, x_k + c_2)\,, \tag{15}$$

one has

$$\left.\frac{\partial F}{\partial p}\right|_{\substack{x=x^o\\p=p^o}} = x^o - (x^o)^2 \quad \text{and} \quad \left.\frac{\partial^2 F}{\partial x^2}\right|_{\substack{x=x^o\\p=p^o}} = -2p^o\,, \tag{16}$$

so that by Table 1,

- if $x^o = 0$ and $p^o \neq 0$, then $(x^o, p^o)$ is a transcritical bifurcating point;
- if $x^o = 0$ and $p^o = 0$, then $(x^o, p^o)$ is a pitchfork bifurcating point;
- if $x^o \neq 0$ and $p^o \neq 0$, then $(x^o, p^o)$ is a saddle-node bifurcating point.

On the other hand, one has

$$\xi = 2(1 - 2x^o) - 2p^o x^o(1 - x^o) \quad \text{and} \quad \eta = 2(p^o)^2\,. \tag{17}$$

Thus, according to Table 5, period-doubling bifurcations with different stabilities of equilibria can be classified for the controlled logistic map. For instance, to shift the original period-doubling bifurcation, starting at a stable equilibrium point $(x^*, p^*) = (2/3, 3)$, see Fig. 1, to a new position, $(x^o, p^o) = (0, -2/3)$, the controller can be designed as described above, and the result is shown in Fig. 9.

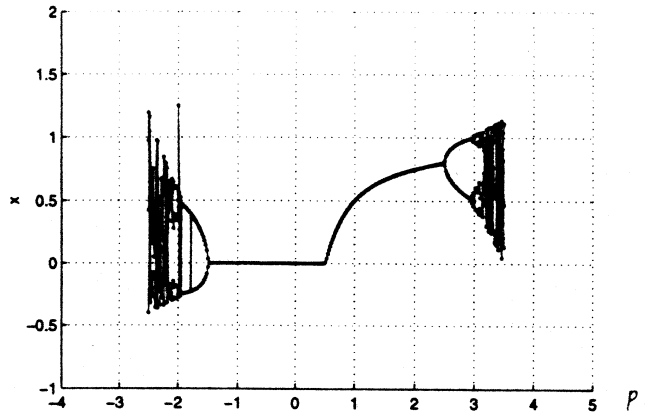


Fig. 9. The controlled period-doubling bifurcation of the Logistic map.

### 5.3. *Controlling the Hopf bifurcation*

Now, consider a Hopf bifurcation control problem, first for continuous-time systems. The objective is to design a simple controller,

$$u(t;\, p) = u(x,\, y;\, p)\,, \tag{18}$$

which does not change the original equilibrium point at $(x^*,\, y^*)$ but can move the Hopf bifurcation point $(x^*,\, y^*,\, p^*)$ to a new position, $(x^o,\, y^o,\, p^o) \neq (x^*,\, y^*,\, p^*)$. Clearly, the controller must satisfy $u(x^*,\, y^*;\, p) = 0$ for all $p$, in order not to change the original equilibrium $(x^*,\, y^*)$.

For the sake of determination, suppose that the controller is added to the second equation of the given system, namely:

$$\begin{cases} \dot{x} = f(x,\, y;\, p) \\ \dot{y} = g(x,\, y;\, p) + u(x,\, y;\, p)\,. \end{cases} \tag{19}$$

This controlled system has the Jacobian at $(x^o,\, y^o)$ as

$$J(p) = \begin{bmatrix} f_x & f_y \\ g_x + u_x & g_y + u_y \end{bmatrix}_{x=x^o,y=y^o}, \tag{20}$$

where $f_x = \partial f/\partial x$ and $g_y = \partial g/\partial y$, etc., with eigenvalues

$$\lambda^c_{1,2}(p) = \frac{1}{2}(f_x + g_y + u_y) \pm \frac{1}{2}\sqrt{(f_x + g_y + u_y)^2 - 4[f_x(g_y + u_y) - f_y(g_x + u_x)]}\,, \tag{21}$$

where $f_x := f_x|_{x=x^o,y=y^o}$ and $g_y := g_y|_{x=x^o,y=y^o}$, etc. for notational simplicity.

To have a Hopf bifurcation at $(x^o,\, y^o;\, p^o)$ as required, the classical Hopf bifurcation theory leads to the following conditions:

(i) $(x^o,\, y^o)$ is an equilibrium point of the controlled system (19), namely,

$$\begin{cases} f(x^o,\, y^o;\, p) = 0 \\ g(x^o,\, y^o;\, p) + u(x^o,\, y^o;\, p) = 0 \end{cases} \tag{22}$$

for all $p \in R$.

(ii) The eigenvalues $\lambda^c_{1,2}(p)$ of the controlled system (19) are purely imaginary at the point $(x^o,\, y^o;\, p^o)$ and are complex conjugate:

$$(f_x + g_y + u_y)|_{p=p^o} = 0\,, \tag{23}$$

$$f_x(g_y + u_y) - f_y(g_x + u_x)|_{p=p^o} > 0\,, \tag{24}$$

$$(f_x + g_y + u_y)^2 - 4[f_x(g_y + u_y) - f_y(g_x + u_x)]|_{p\neq p_0} < 0\,. \tag{25}$$

(iii) The crossing of the eigenlocus at the imaginary axis is transversal, namely,

$$\left.\frac{\partial \mathrm{Re}\{\lambda^c_1(p)\}}{\partial p}\right|_{p=p^o} = \left.\frac{\partial(f_x + g_y + u_y)}{\partial p}\right|_{p=p^o} > 0\,. \tag{26}$$

These conditions provide the guidelines for designing the intended controller [Chen *et al.*, 1999a].

The bifurcation control problem in the discrete-time setting can be carried out in exactly the same way [Chen *et al.*, 1999b]. As an example, for the following one-dimensional time-delayed feedback control system:

$$\begin{cases} x_{k+1} = f(x_k;\, p) + u_k(y_k;\, p) \\ y_{k+1} = x_{k+1} - x_k\,, \end{cases} \tag{27}$$

if the controller is designed to satisfy $u_k(0;\, p) = 0$, then it will not change the original equilibrium point, $x^*$, of the given system. The controlled system has the Jacobian at $(x^o,\, y^o) = (x^*,\, 0)$ as

$$J(p) = \begin{bmatrix} f_x & u_y \\ f_x - 1 & u_y \end{bmatrix}_{x=x^*, y=y^o=0}, \tag{28}$$

where $f_x = \partial f/\partial x_k$ and $u_y = \partial u_k/\partial y_k$, with eigenvalues

$$\lambda_{1,2}(p) = \frac{1}{2}(f_x + u_y) \pm \frac{1}{2}\sqrt{(f_x + u_y)^2 - 4u_y}\,. \tag{29}$$

Conditions for the controller to satisfy $\lambda_1(p) = \bar{\lambda}_2(p)$ and (6) are

$$\begin{gathered} (f_x + u_y)^2 \le 4u_y, \quad |\lambda_{1,2}(p^*)| = 1, \quad \text{and} \\ \frac{\partial |\lambda_{1,2}(p^*)|}{\partial p} > 0\,. \end{gathered} \tag{30}$$

Finally, it should be noted that all the conditions derived in this subsection are necessary conditions for Hopf bifurcations. In order to obtain complete conditions, in both continuous-time and discrete-time cases, one needs to compute a complicated formula to determine the stability of the bifurcated periodic solutions (so as to distinguish the supercritical and the subcritical cases). This formula is called the stability index (or curvature coefficient), and will be further discussed below.

## 6. Various Bifurcation Control Methods

There are some bifurcation control approaches that are not directly derived from the definitions of bifurcations or from the Hopf bifurcation theorem. This section introduces a few of such control techniques, and their implication to the control of oscillations and chaos.

### 6.1. *Bifurcation control via state feedback and washout filter-aided dynamic feedback controllers*

To design a controller for bifurcation modification purpose, Taylor expansion, and sometimes linearization, of the given nonlinear dynamical system is a common approach. Since bifurcations are closely related by the eigenvalues of the linearized model, controlling the behaviors of these eigenvalues in an appropriate way is the key to bifurcation control.

It is fair to state that the field of systematic bifurcation control starts with the work of [Abed & Fu, 1986, 1987], followed by a growing set of results for control of bifurcations of various types [Lee & Abed, 1991; Wang & Abed, 1994, 1995; Chen *et al.*, 1999b]. The work of [Abed & Fu, 1986, 1987] focuses on obtaining stabilizing feedback control laws for general $n$-dimensional one parameter families of nonlinear control systems:

$$\dot{x} = f(x;\, p,\, u)\,. \tag{31}$$

Here, $x$ is the state vector, $u$ is the control input, and $p$ is the bifurcation parameter. The control laws derived in [Abed & Fu, 1986, 1987] transform an unstable (i.e. subcritical) Hopf or stationary bifurcation into a stable (i.e. supercritical) one. These control laws, known as static state feedback, were taken to be of the general form $u = u(x)$. State feedback control laws were designed rendering the assumed Hopf bifurcation or stationary bifurcation locally attracting.

In [Lee & Abed, 1991; Wang & Abed, 1994, 1995], dynamic state feedback control laws incorporating washout filters were developed. In this way, the control laws guarantee preservation of all system equilibria even under model uncertainty.

To illustrate the machinery of bifurcation control, the results of [Abed *et al.*, 1994; Wang & Abed, 1994; Abed & Wang, 1995] are summarized next. Consider a general discrete-time parametric system,

$$\mathbf{x}_{k+1} = \mathbf{f}(\mathbf{x}_k; p)\,, \quad k = 0,\, 1, \ldots, \tag{32}$$

where $\mathbf{f}$ is assumed to be sufficiently smooth, with respect to both $\mathbf{x}_k \in R^n$ and $p \in R$, and has a fixed point at $(\mathbf{x}^*,\, p^*) = (0,\, 0)$.

Assume that system (32) has a fixed point that is the continuous extension of the origin. Suppose

also that the Jacobian of the system, evaluated at this singular point, possesses an eigenvalue, $\lambda_1(p)$, that satisfies $\lambda_1(0) = -1$ and $\lambda_1'(0) \neq 0$, while all remaining eigenvalues have magnitude strictly less than one. Then, the nonlinear function $\mathbf{f}$ has a Taylor expansion,

$$\mathbf{f}(\mathbf{x};\, p) = J(p)\mathbf{x} + \mathbf{q}(\mathbf{x},\, \mathbf{x};\, p) + \mathbf{c}(\mathbf{x},\, \mathbf{x},\, \mathbf{x};\, p) + \cdots ,$$

where $J(p)$ is the parametric Jacobian, and $\mathbf{q}$ and $\mathbf{c}$ are quadratic and cubic vector-valued terms, generated by symmetric bilinear and trilinear forms, respectively.

For this system, the following results [Abed *et al.*, 1994; Wang & Abed, 1994; Abed & Wang, 1995] characterize the bifurcation behavior of the uncontrolled system and provide some guidelines for designing a nonlinear state feedback controller for bifurcation control:

(i) A period-doubling orbit can bifurcate from the origin of system (32) at $p = 0$; the period-doubling bifurcation is supercritical and stable if $\beta < 0$ but is subcritical and unstable if $\beta > 0$, where

$$\beta = 2\,\mathbf{l}^\top[\tilde{\mathbf{c}}(\mathbf{r},\mathbf{r},\mathbf{r};p) - 2\tilde{\mathbf{q}}(\mathbf{r},\tilde{J}^-\tilde{\mathbf{q}}(\mathbf{r},\mathbf{r};p);p)]\,,$$

in which

$\mathbf{l}^\top$ = left eigenvector of $J(0)$ associated with the eigenvalue $-1$

$\mathbf{r}$ = right eigenvector of $J(0)$ associated with the eigenvalue $-1$

$$\tilde{\mathbf{q}} = J(0)\mathbf{q}(\mathbf{x},\, \mathbf{x};\, p) + \mathbf{q}(J(0)\mathbf{x},\, J(0)\mathbf{x};\, p)$$

$$\tilde{\mathbf{c}} = J(0)\mathbf{c}(\mathbf{x},\, \mathbf{x},\, \mathbf{x};\, p) + 2\mathbf{q}(J(0)\mathbf{x},\, \mathbf{q}(\mathbf{x},\, \mathbf{x};\, p);\, p) + \mathbf{c}(J(0)\mathbf{x},\, J(0)\mathbf{x},\, \mathbf{q}(\mathbf{x},\mathbf{x};\, p);\, p)$$

$$\tilde{J}^- = [J^\top(0)J(0) + \mathbf{l}\mathbf{l}^\top]^{-1}J^\top(0)\,.$$

(ii) Consider system (32) with a control input

$$\mathbf{x}_{k+1} = \mathbf{f}(\mathbf{x}_k;\, p,\, \mathbf{u}_k), \quad k = 0,\, 1, \ldots , \tag{33}$$

which is assumed to satisfy the same assumptions as above when $\mathbf{u}_k = 0$. If the critical eigenvalue $-1$ is controllable for the associate linearized system, then there is a feedback control, $\mathbf{u}_k(\mathbf{x}_k)$, containing only third-order terms in the components of $\mathbf{x}_k$, such that the controlled system has a locally stable bifurcated period-two orbit for $p$ near zero. Also, this feedback stabilizes the origin for $p = 0$. If, however, $-1$ is uncontrollable for the associate linearized system, then generically there is a feedback, $\mathbf{u}_k(\mathbf{x}_k)$, containing only second-order terms in the components of $\mathbf{x}_k$, such that the controlled system has a locally stable bifurcated period-two orbit for $p$ near 0. Moreover, this feedback stabilizes the origin for $p = 0$.

As an application, a well-known model of a thermal convection loop can be used to demonstrate the control of bifurcations [Wang & Abed, 1995], where the physical setup of the experiment is shown in Fig. 10. In this setup, the loop is heated from below and cooled from above. This physical system can be described by the Lorenz system

$$\begin{cases} \dot{x} = -p(x - y) \\ \dot{y} = -xz - y \\ \dot{z} = xy - z - r\,, \end{cases} \tag{34}$$

where the state variables, $x$, $y$, and $z$, represent the cross-sectionally averaged velocity in the loop, the temperature difference along the horizontal direction, and the temperature difference along the vertical direction, respectively, as indicated in Fig. 10. In addition, $p > 0$ (Prandtl number) and $r > 0$ (Rayleigh number) are used as parameters.

A bifurcation diagram for this thermal convection model is shown in Fig. 11. In the figure, a solid (resp. a dashed) curve represents a stable (resp. unstable) equilibrium, and "$\circ$" denotes the maximum amplitude of an unstable periodic orbit. The

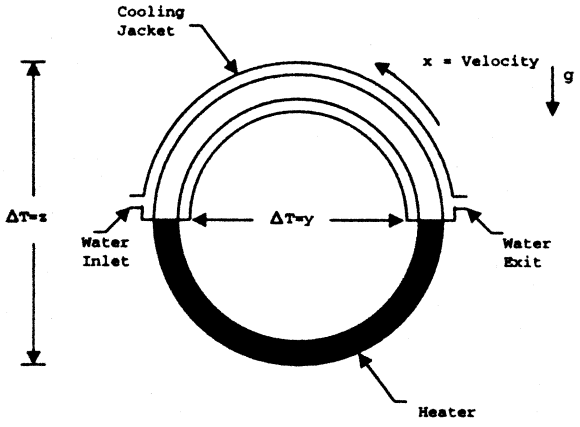


Fig. 10. Structure of the thermal convection loop.

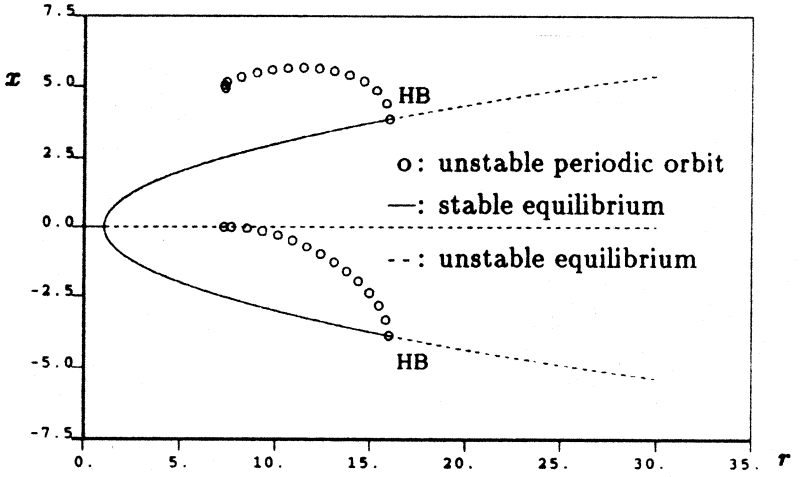


Fig. 11. Bifurcation diagram of the thermal convection loop.

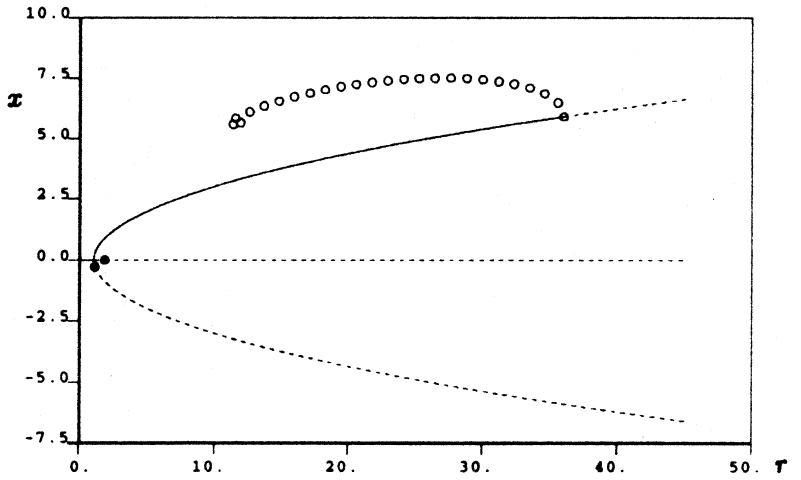


Fig. 12. Bifurcation control in the thermal convection loop.

transient chaotic behavior and chaotic dynamics of the model are shown in Fig. 11 with $r = 14.0$ [Wang & Abed, 1995].

It is well known that the convective equilibria, denoted $C_+$ for the upper loop and $C_-$ for the lower loop of the configuration shown in Fig. 10, lose their stabilities at a Hopf bifurcation occurring at $r = 16.0$. To delay and stabilize the bifurcation, a dynamic feedback control, $u$, utilizing a washout filter, is applied, resulting in

$$\begin{cases} \dot{x} = -p(x - y) \\ \dot{y} = -xz - y \\ \dot{z} = xy - z - r + u \\ \dot{v} = y - c\,v\,, \end{cases} \tag{35}$$

where $v$ is the state of the washout filter used for the control:

$$u = -k_c(y - cv) - k_n(y - cv)^3\,,$$

with constant gains $k_c$ and $k_n$ to be determined in the design, while $c$ is a constant chosen for the filter. Figure 12 shows that with $c = 0.5$, $k_c = 2.5$ and $k_n = 0.009$, a trajectory of the closed-loop controlled system is stabilized [Wang & Abed, 1995].

This bifurcation control technique is important in some time-critical applications, such as in power collapse prevention where a significant delay of bifurcation can be crucial [Wang & Abed, 1993]. This technique also has direct relevance for chaos control [Abed *et al.*, 1994; Wang & Abed, 1994].

### 6.2. *Bifurcation control via normal forms and invariants*

The general theory of bifurcations in nonlinear dynamical systems is built on the basis of normal forms. Systems with the same normal form have equivalent bifurcations. Therefore, bifurcations can be classified according to equivalent systems in normal forms. Thus, development of a systematic design technique for bifurcation control requires a unified basis — a set of normal forms for control systems.

Consider a nonlinear system of the form

$$\dot{\mathbf{x}} = \mathbf{f}(\mathbf{x},\, p) + \mathbf{g}(\mathbf{x},\, p)\mathbf{u}\,, \tag{36}$$

where $\mathbf{f}(0,\, 0) = 0$, $\mathbf{x} \in R^n$ is the state variable, $\mathbf{u} \in R^m$ is the control input, and $p \in R$ is a real variable parameter. System (36) can be reformulated by the following change of coordinates and (regular) state feedback

$$\mathbf{x} = \phi(\mathbf{x},\, p), \quad \mathbf{u} = \alpha(\mathbf{x},\, p) + \beta(\mathbf{x},\, p)\mathbf{u}\,, \quad \beta(0,\, 0) \neq 0\,. \tag{37}$$

A set of normal forms is a family of simple nonlinear control systems, such that any system in the form of (36) can be transformed into a unique system in that family. For dynamical systems without control, Poincaré developed a framework of normal forms for autonomous systems [Wiggins, 1988, 1990]. The normal form theory for control systems differs from the theory of Poincaré in the following two aspects:

(i) In a dynamical system without control, a single vector field is involved. However, there are two vector fields ($\mathbf{f}$ and $\mathbf{g}$) in a controlled system to be simplified simultaneously.
(ii) In the Poincaré theory of normal forms, the transformations used are changes of coordinates. The transformation group for control systems consists of both changes of coordinates and state feedbacks.

Because of these two differences, the study of bifurcations for control systems requires a set of normal forms for both functions $\mathbf{f}$ and $\mathbf{g}$, under the transformation group consisting of changes of coordinates as well as state feedbacks.

The control normal forms obtained in [Kang & Krener, 1992; Kang, 1998a, 1998b] are a set of canonical forms: a system can be transformed into one and only one of a system in such a form. In the following, a system with a single uncontrollable mode is used as an example to illustrate the main idea of the normal form approach in the study of control system bifurcations.

The *equilibrium set* of the system (36) is defined to be

$$E = \{(\mathbf{x},\, p) |\ \exists\ \mathbf{u} = \mathbf{u}_0 \text{ such that } \mathbf{f}(\mathbf{x},\, p) + \mathbf{g}(\mathbf{x},\, p)\mathbf{u}_0 = 0\}\,. \tag{38}$$

If system (36) is not linearly controllable, and if the system has a single uncontrollable mode, $\lambda = 0$, then it can be transformed by (37) into one of the following normal forms:

$$\begin{aligned} \dot{z} &= p + \sum_{i=1}^{n-1} \gamma_{x_i x_i} x_i^2 + \gamma_{z x_1} z x_1 + \gamma_{x_1 p} x_1 p \\ &\quad + \gamma_{zz} z^2 + O(z,\, \mathbf{x},\, p,\, \mathbf{u})^3 \\ \dot{\mathbf{x}} &= A_2 \mathbf{x} + B_2 \mathbf{u} + \tilde{\mathbf{f}}^{[2]}(x) + O(z,\, \mathbf{x},\, p,\, \mathbf{u})^3\,, \end{aligned} \tag{39}$$

or

$$\begin{aligned} \dot{z} &= \sum_{i=1}^{n-1} \gamma_{x_i x_i} x_i^2 + \gamma_{z x_1} z x_1 + \gamma_{x_1 p} x_1 p + \gamma_{zp} z p \\ &\quad + \gamma_{zz} z^2 + \gamma_{pp} p^2 + O(z,\, \mathbf{x},\, p,\, \mathbf{u})^3 \\ \dot{\mathbf{x}} &= A_2 \mathbf{x} + B_2 \mathbf{u} + \tilde{\mathbf{f}}^{[2]}(\mathbf{x}) + O(z,\, \mathbf{x},\, p,\, \mathbf{u})^3\,. \end{aligned} \tag{40}$$

The pair $(A_2,\, B_2)$ is in the Brunovsky controller form, and the vector $\tilde{\mathbf{f}}^{[2]}$ is in the extended controller normal form [Kang & Krener, 1992]. The coefficients in the quadratic terms in (39) and (40) are called *invariants*, which are extremely important in both dynamical analysis and bifurcation control. These invariants are not changeable by transformation (37), and they characterize the nonlinear behavior of the system. The invariants form a matrix:

$$Q = \begin{bmatrix} \gamma_{zz} & \dfrac{\gamma_{z x_1}}{2} & \dfrac{\gamma_{zp}}{2} \\ \dfrac{\gamma_{z x_1}}{2} & \gamma_{x_1 x_1} & \dfrac{\gamma_{x_1 p}}{2} \\ \dfrac{\gamma_{zp}}{2} & \dfrac{\gamma_{x_1 p}}{2} & \gamma_{pp} \end{bmatrix}, \tag{41}$$

where the entries are the corresponding coefficients in the normal forms (39) and (40).

Based on the above normal forms and invariants, the following bifurcation related problems can be easily solved, for the family of systems represented by these normal forms:

(i) The geometry of equilibrium set $E$.
(ii) The types of bifurcations of the systems under a feedback controller.
(iii) The stability of the system under a feedback controller.

For example, system (39) has either a paraboloid-shaped (when $Q_1$ is sign definite) or a saddle-shaped (when $Q_1$ is indefinite with full rank) equilibrium set. It is approximated by

$$p = -[z \quad x_1]Q_1[z \quad x_1]^\top.$$

The importance of the set $E$ is due to the fact that $E$ consists of all the possible equilibria of a closed-loop system. In fact, if a state feedback $\mathbf{u} = \alpha(\mathbf{x})$ is applied to the system in normal form, the set of closed-loop equilibria is the intersection between $\alpha(\mathbf{x}) = 0$ and the set $E$. Since $E$ is a paraboloid or a saddle, the intersection is a parabola. This implies that the closed-loop system has a saddle-node bifurcation.

The stability of the system around the saddle-node bifurcation can also be determined by the invariants. In fact, the closed-loop system is locally asymptotically stable about an equilibrium, $(z, x_1, p) \in E_c$ if

$$[a_1 \quad -a_z \quad 0]Q[z \quad x_1 \quad p]^\top > 0\,,$$

where $a_1$ and $a_z$ are the coefficients of $x_1$ and $z$ in the feedback controller $\mathbf{u}(\mathbf{x})$. The related mathematical details can be found in [Kang & Krener, 1992; Kang, 1998a, 1998b].

### 6.3. *Bifurcation control via harmonic balance approximations*

For continuous-time systems, limit cycles generally do not have analytic forms, and so have to be approximated in applications. For this purpose, the harmonic balance approximation technique is very efficient. This technique is useful in controlling bifurcations [Basso *et al.*, 1998], such as for delaying and stabilizing the onset of period-doubling bifurcations [Genesio *et al.*, 1993; Tesi *et al.*, 1996].

Consider the Lur'e system described by

$$\mathbf{f} * (\mathbf{g} \circ \mathbf{y} + K_c \circ \mathbf{y}) + \mathbf{y} = 0\,, \tag{42}$$

where $*$ and $\circ$ represent the convolution and composition operations, respectively. For a given system, $S = S(\mathbf{f}, \mathbf{g})$, as shown in Fig. 13 without the feedback control loop of $K_c$, assume that two

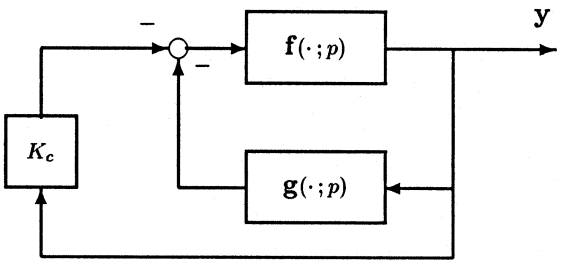


Fig. 13. The closed-loop Lur'e system.

parameters, $p_h$ and $p_c$, are specified, which define a Hopf bifurcation and a supercritical predicted period-doubling bifurcation, respectively. Suppose also that the system has a family of predicted first-order limit cycles, which are stable within the range $p_h < p < p_c$.

The objective here is to design a feedback controller with gain $K_c$ such that the controlled system, $S^* = S^*(\mathbf{f}, \mathbf{g}, K_c)$, has the following properties [Tesi *et al.*, 1996]:

(i) $S^*$ has a Hopf bifurcation for $p_h^* = p_h$;
(ii) $S^*$ has a supercritical predicted period-doubling bifurcation for $p_c^* > p_c$;
(iii) $S^*$ has a one-parameter family of stable predicted limit cycles for $p_h^* < p < p_c^*$;
(iv) $S^*$ has the same set of equilibria as $S$.

As an illustrative example, consider a simple one-dimensional case where a washout filter with the transfer function $s/(s+a)$ $(a > 0)$ is used. Since a predicted first-order limit cycle can be approximated by

$$y_{[1]}(t) = y_0 + y_1 \sin(\omega t)\,,$$

the controller transfer function can take on the form

$$K_c(s) = k_c \frac{s(s^2 + \omega^2(p_h))}{(s+a)^3}\,,$$

where $k_c$ is a constant gain to be designed, $\omega = \omega(p_h)$ is the frequency of the limit cycle emerged from the Hopf bifurcation at the point $p = p_h$. This controller preserves the Hopf bifurcation at the same point. More importantly, since $a > 0$, the controller is stable, so that by continuity in a neighborhood of the nominal value $k_c = 0$, the Hopf bifurcation of $S^*$ not only remains supercritical but also has a supercritical predicted period-doubling

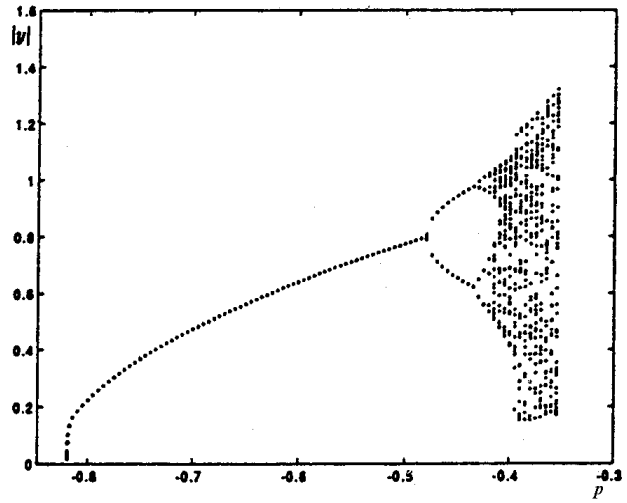


(a) before control

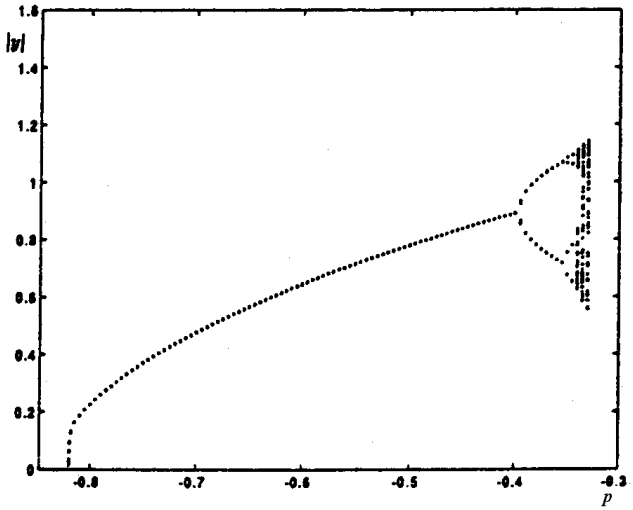


(b) after control

Fig. 14. Bifurcation delay via the harmonic balance technique.

bifurcation (say at $p_c(k_c)$, close to $p_h$) and a one-parameter family of stable predicted limit cycles, for $p_h < p < p_c(k_c)$.

Finally, to determine $k_c$ such that the predicted period-doubling bifurcation can be delayed to a desired parameter value, $p_c^*$, the following harmonic balance equation

$$\begin{cases} y_0[1 + G(0)\, k_0(y_0, y_1)] = 0 \\ 1 + G(j\omega)K_c(j\omega) + G(j\omega)k_1(y_0,\, y_1) = 0\,, \end{cases}$$

is solved, where $G$ is the transfer function of the linearized plant, $f'$. These two equations are solved for $y_0^*$, $y_1^*$, and $\omega^*$, as functions of $p$, depending on $k_c$ and $a$, within the range $p_h < p < p_c^*$. For the period-doubling prediction to occur at the point $p_c^*$, the following condition must be satisfied:

$$\begin{aligned} &1 + H(j\omega^*(p_c^*/2))K_c(j\,\omega^*(p_c^*/2)) \\ &\quad + H(j\omega^*(p_c^*/2))k_{1/2}(y_0(p_c^*),\, y_1(p_c^*),\, \phi) = 0\,, \end{aligned} \tag{43}$$

where $k_{1/2}$ is the describing function of the linearized $g$ at period-doubling and $\phi$ is the related phase of the subharmonic term. Thus, by numerically solving for $k_c$, $a$, and $\phi$, a stable predicted period-doubling can be guaranteed at $p = p_c^*$. Moreover, for each $p \in (p_h,\, p_c^*)$, the predicted limit cycle is stable [Tesi *et al.*, 1996]. For a system with

$$g(y) = -y^2\,.$$

and

$$G(s) = \frac{1}{s^3 + \alpha s^2 + 1.2s + 1}\,,$$

where $p = -\alpha < 0$ is chosen to specify the bifurcation, the controller is found to be

$$K_c(s) = 0.43\,\frac{s(s^2 + 1.2)}{(s+1)^3}\,.$$

This achieves all the expected goals of control listed above, and changes the period-doubling point from $p = -0.48$ to $p = -0.39$, thereby delaying the chaotic motion of the system (see Fig. 14).

## 7. Controlling Hopf Bifurcations

As seen from the previous sections, limit cycles are associated with bifurcations. In fact, one type of degenerate (or singular) Hopf bifurcations determines the appearance of multiple limit cycles under system parameter variation. Therefore, the birth and the amplitudes of multiple limit cycles can be controlled by monitoring the corresponding degenerate Hopf bifurcations [Berns *et al.*, 1998a; Moiola & Chen, 1998; Calandrini *et al.*, 1999]. This task can be accomplished in the frequency domain setting.

### 7.1. *Graphical Hopf bifurcation theorem*

Consider a general parametrized autonomous nonlinear system in the Lur'e form:

$$\begin{cases} \dot{\mathbf{x}} = A(p)\mathbf{x} + B(p)\mathbf{u} \\ \mathbf{y} = -C(p)\mathbf{x} \\ \mathbf{u} = \mathbf{g}(\mathbf{y};\, p)\,, \end{cases} \tag{44}$$

where the matrix $A(p)$ is invertible for all values of parameter $p$. Assume that this system has an equilibrium solution, $\mathbf{y}^*$, satisfying

$$\mathbf{y}^*(p) = -G(0;\, p)\mathbf{g}(\mathbf{y}^*(p);\, p)\,, \tag{45}$$

where

$$G(0;\, p) = -C(p)A^{-1}(p)B(p)\,.$$

Let $J(p) = \partial\mathbf{g}/\partial\mathbf{y}|_{\mathbf{y}=\mathbf{y}^*}$ and let $\check{\lambda} = \check{\lambda}(j\omega;\, p)$ be the eigenvalue of the matrix

$$G(s;\, p)|_{s=j\omega}J(p) = C(p)[j\omega I - A(p)]^{-1}B(p)J(p)$$

that is closest to the critical point which satisfies

$$\check{\lambda}(j\omega_0;\, p_0) = -1 + j0, \quad j = \sqrt{-1}\,.$$

Fix $p = \tilde{p}$ and let $\omega$ vary. Then a trajectory of the function $\check{\lambda}(\omega;\, \tilde{p})$ (the "eigenlocus") can be obtained. This locus traces out from the frequency $\omega_0 \neq 0$. In much the same way, a real zero eigenvalue (a condition for the *static bifurcation*) is replaced by a characteristic gain locus that crosses the point $(-1+j0)$ at frequency $\omega_0 = 0$.

### 7.1.1. *The single-input single-output case*

In particular, for SISO systems, the matrix $[G(j\omega;\, p)J(p)]$ is merely a scalar, so that

$$y(t) \approx y^* + \Re\left\{\sum_{k=0}^{n} y_k e^{jk\omega t}\right\}, \tag{46}$$

where the complex coefficients $\{y_k\}$ are determined as follows. For the approximation with $n = 2$, say, define an auxiliary vector:

$$\xi_1(\tilde{\omega}) = \frac{-\mathbf{l}^\top[G(j\tilde{\omega};\, \tilde{p})]\mathbf{h}_1}{\mathbf{l}^\top\mathbf{r}}\,, \tag{47}$$

where $\tilde{p}$ is the fixed value of parameter $p$, $\mathbf{l}^\top$ and $\mathbf{r}$ are the left and right eigenvectors of $[G(j\tilde{\omega};\, \tilde{p})J(\tilde{p})]$, respectively, associated with the eigenvalue $\check{\lambda}(j\tilde{\omega};\, \tilde{p})$, and

$$\mathbf{h}_1 = \left[D_2\left(\mathbf{z}_{02}\otimes\mathbf{r} + \frac{1}{2}\bar{\mathbf{r}}\otimes\mathbf{z}_{22}\right) + \frac{1}{8}D_3\mathbf{r}\otimes\mathbf{r}\otimes\bar{\mathbf{r}}\right], \tag{48}$$

in which $\bar{\cdot}$ denotes the complex conjugate, $\tilde{\omega}$ is the frequency of the intersection between the $\check{\lambda}$ locus and the negative real axis, closest to the point $(-1+j0)$, $\otimes$ is the tensor product operator, and

$$D_2 = \left.\frac{\partial^2\mathbf{g}(y;\, \tilde{p})}{\partial y^2}\right|_{y=y^*}, \quad D_3 = \left.\frac{\partial^3\mathbf{g}(y;\, \tilde{p})}{\partial y^3}\right|_{y=y^*}$$

$$\mathbf{z}_{02} = -\frac{1}{4}[1 + G(0;\, \tilde{p})J(\tilde{p})]^{-1}G(0;\, \tilde{p})D_2\mathbf{r}\otimes\bar{\mathbf{r}}$$

$$\mathbf{z}_{22} = -\frac{1}{4}[1 + G(2j\tilde{\omega};\, \tilde{p})J(\tilde{p})]^{-1}G(2j\tilde{\omega};\, \tilde{p})D_2\mathbf{r}\otimes\mathbf{r}$$

$$y_0 = \mathbf{z}_{02}|\tilde{p} - p_0|, \quad y_1 = \mathbf{r}|\tilde{p} - p_0|^{1/2},$$

$$y_2 = \mathbf{z}_{22}|\tilde{p} - p_0|\,.$$

Furthermore, the stability index (or curvature coefficient), which indicates the stability of the emerging limit cycle, has the following expression:

$$\sigma_1(\omega_0) = -\mathrm{Re}\left\{\frac{\mathbf{l}^\top[G(\omega_0;\, p_0)]\mathbf{h}_1}{\mathbf{l}^\top G'(\omega_0;\, p_0)J(p_0)\mathbf{r}}\right\}, \tag{49}$$

where $G'(\omega_0;\, p_0) = \left.\frac{dG(s)}{ds}\right|_{\omega=\omega_0, p=p_0}$.

Then, the graphical Hopf bifurcation theorem (for SISO systems), formulated in the frequency domain, can be stated as follows [Mees & Chua, 1979; Moiola & Chen, 1996]:

**Theorem** (Graphical Hopf Bifurcation Theorem). *Suppose that when $\omega$ varies, the vector $\xi_1(\tilde{\omega}) \neq 0$, and the half-line, starting from $-1 + j0$ and pointing to the direction parallel to that of $\xi_1(\tilde{\omega})$, first intersects the locus of the eigenvalue $\check{\lambda}(j\omega;\, \tilde{p})$, at the point*

$$\check{P} = \check{\lambda}(\check{\omega};\, \tilde{p}) = -1 + \xi_1(\tilde{\omega})\theta^2\,,$$

*at which $\omega = \check{\omega}$ and the constant $\theta = \theta(\tilde{\omega}) \geq 0$, as shown in Fig. 15. Suppose, furthermore, that the above intersection is transversal, namely,*

$$\det\begin{bmatrix} \Re\{\xi_1(j\tilde{\omega})\} & \Im\{\xi_1(j\tilde{\omega})\} \\ \Re\left\{\dfrac{d}{d\omega}\check{\lambda}(\omega;\, \tilde{p})\Big|_{\omega=\check{\omega}}\right\} & \Im\left\{\dfrac{d}{d\omega}\check{\lambda}(\omega;\, \tilde{p})\Big|_{\omega=\check{\omega}}\right\} \end{bmatrix} \neq 0\,.$$

*Then*

(i) *The nonlinear system (44) has a periodic solution (output) $y(t) = y(t;\, y^*)$. Consequently, there exists a unique limit cycle for the nonlinear equation $\dot{\mathbf{x}} = \mathbf{f}(\mathbf{x})$, in a ball of radius $O(1)$ centered at the equilibrium $\mathbf{x}^*$.*

(ii) *If the total number of counterclockwise encirclements of the point $p_1 = \check{P} + \varepsilon\xi_1(\tilde{\omega})$, for a small enough $\varepsilon > 0$, is equal to the number of poles of $[G(s;\, p)J(p)]$ that have positive real parts, then the limit cycle is stable.*

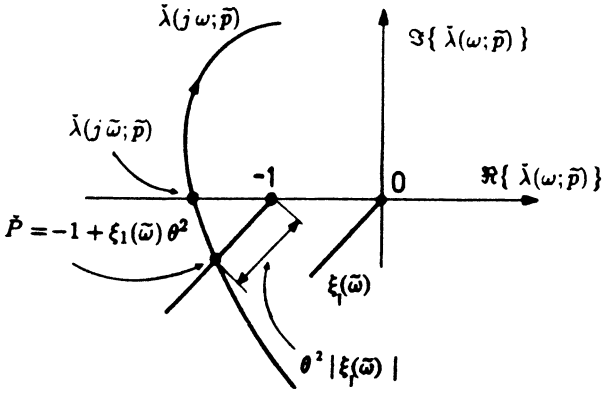


Fig. 15. The frequency-domain Hopf bifurcation theorem.

### 7.1.2. *An example of Hopf bifurcation control*

Consider the following system:

$$\begin{aligned}\dot{x}_1 &= -x_1x_2 + x_2^2 + p\,,\\ \dot{x}_2 &= -x_2 + x_1^3 + px_2\,,\end{aligned} \tag{50}$$

where $p$ plays the role of the main bifurcation parameter, which can be viewed as the input to the planar system. This system can be transformed into the required format, with

$$G(s) = \begin{bmatrix} \dfrac{1}{s+\alpha} & 0 \\ 0 & \dfrac{1}{s+1}\end{bmatrix}$$

and

$$g(y,\,p) = \begin{bmatrix} -y_1y_2 + y_2^2 + p - \alpha y_1 \\ -y_1^3 - py_2\end{bmatrix},$$

by choosing

$$A = \begin{bmatrix} -\alpha & 0 \\ 0 & -1\end{bmatrix} \quad \text{and} \quad B = C = I_2\,,$$

where the constant $\alpha > 0$ is introduced to guarantee the open-loop system poles being located in the left-half plane. The equilibrium points of the system are obtained as follows:

$$\begin{aligned}\frac{1}{\alpha}[-y_1^*y_2^* + (y_2^*)^2 + p - \alpha y_1^*] &= -y_1^* \\ \Rightarrow -y_1^*y_2^* + (y_2^*)^2 + p &= 0\,,\end{aligned} \tag{51}$$

$$-(y_1^*)^3 - py_2^* = -y_2^*\,. \tag{52}$$

Note that for $p = 0$, one has

$$P_I = (y_1^*,\, y_2^*)_1 = (0,\, 0)$$

and

$$P_{II,III} = (y_1^*,\, y_2^*)_2 = (\pm 1,\, \pm 1)\,.$$

The system Jacobian is

$$J = \begin{bmatrix} -y_2^* - \alpha & -y_1^* + 2y_2^* \\ -3(y_1^*)^2 & -p\end{bmatrix} \tag{53}$$

and the characteristic gain loci are

$$\begin{aligned}&\lambda^2 + \lambda\left(\frac{p}{s+1} + \frac{y_2^* + \alpha}{s+\alpha}\right)\\ &\quad + \frac{p(y_2^* + \alpha) - 3(y_1^*)^2(y_1^* - 2y_2^*)}{(s+1)(s+\alpha)} = 0\,.\end{aligned} \tag{54}$$

When $\check{\lambda} = -1$ (a single root) and $s = i\omega$, one obtains the general bifurcation condition, as

$$1 - \frac{[(j\omega+\alpha)p + (y_2^*+\alpha)(1+j\omega)] - p(y_2^*+\alpha) + 3(y_1^*)^2(y_1^* - 2y_2^*)}{(1+j\omega)(\alpha+j\omega)} = 0\,. \tag{55}$$

If $\omega_0 = 0$ satisfies Eq. (55), one obtains a condition, for static bifurcations, as

$$y_2^*(p-1) + 3(y_1^*)^2(2y_2^* - y_1^*) = 0\,. \tag{56}$$

Next, rewriting Eq. (52) as

$$\frac{(y_1^*)^3}{(1-p)} = y_2^*\,, \tag{57}$$

and replacing $y_2^*$ by this expression in Eq. (56), one obtains

$$y_{1sb}^{*(1)} = 0 \quad \text{and} \quad y_{1sb}^{*(2,3)} = \pm\sqrt{\frac{2}{3}(1-p)}\,.$$

Substituting this expression into Eq. (57) gives

$$y_{2sb}^{*(1)} = 0 \quad \text{and} \quad y_{2sb}^{*(2,3)} = \pm\frac{2}{3}\sqrt{\frac{2}{3}(1-p)}\,.$$

Finally, replacing the expressions of $y_1^{*(1,2,3)}$ and $y_2^{*(1,2,3)}$ in Eq. (51), one obtains the values of $p$ that give the following (saddle-node type) static bifurcation points:

$$p_{0sb} = 0, \quad P_{I_{sb}} = (y_1^*,\, y_2^*)_{1_{sb}} = (0,\, 0)\,,$$

$$p_{1sb} = \frac{4}{31}\,,$$

$$P_{II_{sb},III_{sb}} = (y_1^*,\, y_2^*)_{2_{sb},3_{sb}} = \left(\pm 3\sqrt{\frac{2}{31}},\, \pm 2\sqrt{\frac{2}{31}}\right).$$

If $\omega_0 \neq 0$ satisfies Eq. (55), one has a condition for the Hopf bifurcation. So, let $\alpha = 1$ for simplicity. After separating Eq. (55) in real and imaginary parts, one has

$$-\omega_0^2 + y_2^*(p-1) + 3(y_1^*)^2(2y_2^* - y_1^*) = 0\,,$$

$$\omega_0(1-p) = y_2^*\omega_0 \Rightarrow y_2^* = (1-p)\,.$$

To this end, applying Eqs. (51) and (52) into this last equation yields

$$-2p + 4p^2 - 3p^3 - p^4 + 2p^5 - p^6 = 0\,. \qquad (58)$$

Note that there are only two real roots of $p$ that satisfy Eq. (58), and they are the bifurcating values for Hopf bifurcations:

(a) HB1

$$p_{\mathrm{HB1}} = 0, \quad (y_1^*,\, y_2^*)_{\mathrm{HB1}} = (1,\, 1), \quad \omega_{01} = \sqrt{2}\,,$$

(b) HB2

$$p_{\mathrm{HB2}} = -1.32471795,$$

$$(y_1^*,\, y_2^*)_{\mathrm{HB2}} = (1.7548775,\, 2.32471795),$$

$$\omega_{02} = 4.6192952\,.$$

One can then analyze the stability of the equilibrium solutions by using small perturbations around the bifurcation points, and check if any one of the characteristic loci [Eq. (54)] encircles the critical point $(-1 + i0)$. To obtain complete results, however, it is preferred to find the directions of periodic solutions starting from the criticality, i.e. the stability of the emerging periodic branch. Here, for simplicity, only HB1 is discussed.

The right and left normalized eigenvectors ($\mathbf{l}^\top\mathbf{r} = \mathbf{1}$, $|\mathbf{r}| = \mathbf{1}$) of the matrix $[G(j\omega_{01})J]$ belonging to $\breve{\lambda} = -1$ are

$$\mathbf{r} = \begin{pmatrix} \dfrac{1}{2} \\ \dfrac{1}{2} - j\dfrac{\sqrt{2}}{2} \end{pmatrix} \quad \text{and} \quad \mathbf{l}^\top = \begin{pmatrix} 1 - \dfrac{j}{\sqrt{2}} & \dfrac{j}{\sqrt{2}} \end{pmatrix}.$$

By using the formulas given above (evaluated at criticality $\omega_{01} = \sqrt{2}$), one has

$$\mathbf{z}_{02} = -\frac{1}{16}\begin{bmatrix} 5 \\ 9 \end{bmatrix}, \quad \mathbf{z}_{22} = \frac{1}{24}\begin{bmatrix} \dfrac{5}{2} - 5\dfrac{\sqrt{2}}{2}j \\ -\dfrac{3}{2} - 9\dfrac{\sqrt{2}}{2}j \end{bmatrix},$$

$$\mathbf{h}_1 = \frac{1}{16}\begin{bmatrix} -\dfrac{1}{2} + 21\dfrac{\sqrt{2}}{4}j \\ 11 + 5\dfrac{\sqrt{2}}{2}j \end{bmatrix},$$

which gives a very simple formula for the stability index $\sigma_1(\omega_{01}) = -9/64$. This corresponds to a stable periodic solution emerging from the first Hopf bifurcation point. Equivalent computations show that the second Hopf bifurcation point HB2 also has a negative stability index and, hence, a stable periodic solution is associated with it.

## 7.2. *Controlling the birth of multiple limit cycles*

As mentioned earlier, one type of degenerate Hopf bifurcations determine the appearance of multiple limit cycles under system parameter variation. The birth of multiple limit cycles can be controlled on the basis of this intrinsic connection, by modifying the corresponding degenerate Hopf bifurcations via parameter variations.

### 7.2.1. *Necessary conditions for multiple limit cycles*

For the harmonic expansion of (46) with higher-order approximations ($n > 2$), more accurate formulas can be derived. In particular, the first harmonic of the output $y(t)$ is obtained as

$$\mathbf{y}^{[1]} = \theta\mathbf{r} + \theta^3\mathbf{z}_{13} + \theta^5\mathbf{z}_{15} + \cdots\,, \qquad (59)$$

where $\mathbf{z}_{13}, \ldots, \mathbf{z}_{1,2m+1}$ are vectors orthogonal to $\mathbf{r}$, $m = 1, 2, \ldots$, which can be explicitly calculated [Moiola & Chen, 1996].

For a given value of $\breve{\omega}$, which is the approximation of the oscillatory frequency,

$$G(j\breve{\omega}) = G(s) + (-\alpha + j\delta\omega)G'(s) + \frac{1}{2}(-\alpha + j\delta\omega)^2 G''(s) + \cdots\,, \qquad (60)$$

where $\delta\omega = \breve{\omega} - \omega$, in which $\omega$ is the imaginary part of the bifurcating eigenvalues, and $G'(s)$ and $G''(s)$ are the first and second derivatives of $G(s)$, respectively, with respect to $s$.

On the other hand, with the higher-order approximations, one has

$$[G(j\omega)J + I]\sum_{i=0}^{m} \mathbf{z}_{1,2i+1}\theta^{2i+1} = -G(j\omega)\sum_{i=1}^{m} \mathbf{v}_{1,2i+1}\theta^{2i+1}, \quad (61)$$

where $\mathbf{z}_{11} = \mathbf{r}$ and $\mathbf{v}_{1,2m+1} = \mathbf{h}_m$, $m = 1, 2, \ldots$, with explicit formulas for computation [Moiola & Chen, 1996].

In a general situation, the following equation has to be solved:

$$[G(j\breve{\omega})J + I](\mathbf{r}\theta + \mathbf{z}_{13}\theta^3 + \mathbf{z}_{15}\theta^5 + \cdots) = -G(j\breve{\omega})[\mathbf{h}_1\theta^3 + \mathbf{h}_2\theta^5 + \cdots]. \quad (62)$$

To do so, by substituting (60) into (62), one obtains

$$(\alpha - j\delta\omega) = \gamma_1\theta^2 + \gamma_2\theta^4 + \gamma_3\theta^6 + \gamma_4\theta^8 + O(\theta^9), \quad (63)$$

in which all coefficients, $\gamma_i$, $i = 1, 2, 3, 4$, can be calculated explicitly [Moiola & Chen, 1996].

Then, taking the real part of (63) gives

$$\alpha = -\sigma_1\theta^2 - \sigma_2\theta^4 - \sigma_3\theta^6 - \sigma_4\theta^8 - \cdots, \quad (64)$$

where $\sigma_i = -\Re\{\gamma_i\}$ are the *stability index* or *curvature coefficients* of the expansion. In the terminology of degenerate Hopf bifurcation, the degeneracies are denoted as $H_{ij}$. Here, in $H_{ij}$, the subscript $i$ indicates that the stability index vanish at criticality up to the $i$th order, while $j$ means the order in which the derivative(s) for the failure of the transversality condition vanishes. Thus, $H_{00}$ is the classical Hopf bifurcation without any degeneracy in the transversality condition.

Note that multiple limit cycles arise when the stability indexes are perturbed near the value zero, after the signs of the stability indexes are altered in an increasing (or decreasing) order. For example, to have four limit cycles in the vicinity of an $H_{30}$-degenerate Hopf bifurcation, (i.e. at the criticality, $\sigma_1 = \sigma_2 = \sigma_3 = 0$ but $\sigma_4 \neq 0$), the system parameters have to be perturbed in such a way that their signs are alternating, say, $\alpha > 0$, $\sigma_1 < 0$, $\sigma_2 > 0$, $\sigma_3 < 0$, and $\sigma_4 > 0$ [Calandrini *et al.*, 1999].

### 7.2.2. *An example of multiple limit cycle control*

Consider a planar cubic system in the Lur'e form (44), with

$$A = \begin{bmatrix} -1 & 0 \\ 0 & -1 \end{bmatrix}, \quad B = C = \begin{bmatrix} 1 & 0 \\ 0 & 1 \end{bmatrix},$$

$$G(s) = \begin{bmatrix} \dfrac{1}{(s+1)} & 0 \\ 0 & \dfrac{1}{(s+1)} \end{bmatrix},$$

$$J = \begin{bmatrix} -(p+1) & 1 \\ -1 & -(p+1) \end{bmatrix},$$

and

$$\mathbf{g}(\mathbf{y}) = \begin{bmatrix} -(p+1)y_1 + y_2 - (a-w-\beta)y_1^3 - (3\mu-\eta)y_1^2y_2 \\ -(3\beta+\xi-3w-2a)y_1y_2^2 - (q-\mu)y_2^3 \\ -y_1 - y_2(p+1) - (q+\mu)y_1^3 - (3w+3\beta+2a)y_1^2y_2 \\ -(\eta-3\mu)y_1y_2^2 - (w-\beta-a)y_2^3 \end{bmatrix},$$

where $p$ plays the role of the main bifurcation parameter and $a$, $w$, $\beta$, $\mu$, $\eta$, $\xi$ and $q$, are system parameters, and $\mathbf{y} = -\mathbf{x} = -[x_1x_2]^\top$. For this system,

$$\mathbf{r} = \begin{bmatrix} \dfrac{1}{\sqrt{2}} \\ -\dfrac{j}{\sqrt{2}} \end{bmatrix}, \quad \mathbf{l} = \begin{bmatrix} \dfrac{1}{\sqrt{2}} \\ \dfrac{j}{\sqrt{2}} \end{bmatrix},$$

and

$$\mathbf{y}^* = \mathbf{z}_{02} = \mathbf{z}_{22} = 0.$$

Moreover, the first three stability indexes are

$$\sigma_1 = \frac{1}{16}\xi, \quad \sigma_2 = -\frac{5}{32}aq, \quad \text{and} \quad \sigma_3 = \frac{25}{128}aw\beta.$$

To control the birth of multiple limit cycles from this system, choose a parameter, $\xi < 0$, so that the first stability index has a definite sign. This yields a stable periodic solution at the Hopf bifurcation point. Moreover, from the expression of $\sigma_2$, one can see that the values of the parameters $a$ and $q$ must have the same sign, to ensure $\sigma_2 < 0$. Finally, from the formula of $\sigma_3$, which depends on parameters $a$, $\omega$ and $\beta$, it is clear that to ensure a negative sign for $\sigma_3$, there are four possibilities:

(1) $\text{sgn}\,[a] = -1$, $\text{sgn}\,[\omega] = 1$ and $\text{sgn}\,[\beta] = 1$.
(2) $\text{sgn}\,[a] = 1$, $\text{sgn}\,[\omega] = -1$ and $\text{sgn}\,[\beta] = 1$.
(3) $\text{sgn}\,[a] = 1$, $\text{sgn}\,[\omega] = 1$ and $\text{sgn}\,[\beta] = -1$.
(4) $\text{sgn}\,[a] = -1$, $\text{sgn}\,[\omega] = -1$ and $\text{sgn}\,[\beta] = -1$.

One advantage of this methodology is that feedback control (e.g. adding any nonlinear terms) is not needed: one can simply modify the system parameters according to the expressions of the stability indexes, to achieve the goal of controlling the birth of multiple limit cycles (for more details, see [Moiola & Chen, 1998; Calandrini *et al.*, 1999]). A more complex system with multiple oscillations has been analyzed in [Berns & Moiola, 1998] giving at the same time a procedure to locate in the parameter space the singularities of higher-order codimension. Furthermore, multiple periodic solutions have been detected in aircraft lateral dynamics [Ananthkrishnan & Sudhakar, 1996], in which the presence of large periodic solutions provokes adverse effects on maneuverability of the aircraft, and hence its control is of fundamental and critical importance.

### 7.3. *Controlling the amplitudes of limit cycles*

Consider the parametrized nonlinear system (44), with one more parameter, $\alpha$, in the form

$$\begin{cases} \dot{x}(t) = A(p,\,\alpha)x(t) + B(p,\,\alpha)g(C(p,\,\alpha)x(t);\,p,\,\alpha) \\ y(t) = C(p,\,\alpha)x(t)\,, \end{cases} \tag{65}$$

where $A, B$, and $C$ are $n \times n$, $n \times r$ and $m \times n$ matrices, respectively, $p \in R$ and $\alpha \in R$ are the main and auxiliary bifurcation parameters, respectively, $x \in R^n$ is the state vector, $y \in R^\ell$ is the system output, and the smooth nonlinear function $g$: $R^\ell \to C^{2r+1}(R^r)$ is considered as the system input.

Taking Laplace transforms on (65) yields

$$(\mathcal{L}e)(s) = -G(s;\,p,\,\alpha)(\mathcal{L}u)(s)\,, \tag{66}$$

where

$$e(t) = -y(t) = -Cx(t)$$
$$G(s;\,p,\,\alpha) = C\,[sI - A]^{-1}\,B$$
$$u(t) = g(Cx(t);\,p,\,\alpha) := f(e(t);\,p,\,\alpha)\,.$$

The equilibrium solution of (66), $e^*$, can be obtained by solving the equation

$$G(0;\,p,\,\alpha)f(e^*;\,p,\,\alpha) = -e^*\,. \tag{67}$$

Consider the characteristic equation

$$\det\,[\lambda I - G(s;\,p,\,\alpha)J] = \lambda^m + a_{m-1}(s;\,p,\,\alpha)\lambda^{m-1} + \cdots + a_0(s;\,p,\,\alpha) = 0\,,$$

where $J = \partial f/\partial e|_{e=e^*}$ is the Jacobian, and $m = \min(\ell,\,r)$. Letting $s = j\omega$ and using the bifurcation condition $\check{\lambda} = -1$, the above equation is separated into real and imaginary parts:

$$F_1(\omega,\,p,\,\alpha) = (-1)^m + \sum_{k=0}^{m-1}(-1)^k \Re\,\{a_k(j\omega;\,p,\,\alpha)\} = 0$$

$$F_2(\omega,\,p,\,\alpha) = \sum_{k=0}^{m-1}(-1)^k \Im\,\{a_k(j\omega;\,p,\,\alpha)\} = 0\,,$$

Hopf bifurcation points are found from the solutions of these two equations, which are denoted $(\omega_0,\,p_0,\,\alpha_0)$, provided that $\omega_0 \neq 0$.

A regular Hopf bifurcation point is a partial solution of the above two equations, which is denoted $(\omega_0,\,\alpha_0)$ and satisfies

$$\det \begin{bmatrix} \dfrac{\partial F_1}{\partial p} & \dfrac{\partial F_2}{\partial p} \\ \dfrac{\partial F_1}{\partial \omega} & \dfrac{\partial F_2}{\partial \omega} \end{bmatrix}_{(\omega_0,\alpha_0)} \neq 0,$$

where $\frac{\partial F_1}{\partial \omega} \neq 0$ and $\frac{\partial F_2}{\partial \omega} \neq 0$, at $(\omega_0,\,\alpha_0)$, and

$$\det \begin{bmatrix} \Re\{\xi_1(\omega)\} & \Im\{\xi_1(\omega)\} \\ \Re\left\{\dfrac{d\check{\lambda}}{d\omega}\right\} & \Im\left\{\dfrac{d\check{\lambda}}{d\omega}\right\} \end{bmatrix}_{(\omega_0,\alpha_0)} = \sigma_1(\omega_0,\,\alpha_0) \neq 0.$$

Here, $\xi_1$ is a complex number depending on the second and third orders of partial derivatives of the function $f(e(t))$, evaluated at $e^*$; $\check{\lambda}$ is the eigenvalue closest to the critical point $(-1 + j0)$ when $s = j\omega$ is sweeping onto the Nyquist contour; and $\sigma_1(\cdot)$ is the first stability index.

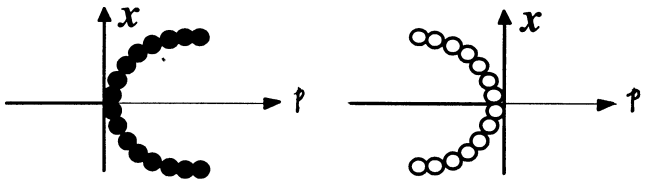


Fig. 16. Classical Hopf bifurcation: supercritical and subcritical. Black dots correspond to stable limit cycles while circles represent unstable limit cycles.

### 7.3.1. *Degenerate Hopf bifurcations and control of oscillations*

Next, consider a periodic solution of (66), $y(t)$, given by its $2m$th-order approximation

$$y(t) \approx y^* + \Re\left\{\sum_{k=0}^{2m} Y^k\, e^{jk\omega t}\right\}, \qquad (68)$$

where $Y^k$ is a complex number in the $k$th harmonic of the expansion. These $\{Y^k\}$ are obtained after equating the output of the linear part of the system, $-G(jk\omega)F^k$, with the input signal to the nonlinear feedback function $f(e) := g(y)$ that has Fourier coefficients $\{F^k\}$. Then, the following harmonic balance equations is obtained:

$$Y^k = -G(jk\omega,\, p,\, \alpha)F^k(Y^k,\, Y^{k-1}, \ldots,\, Y^0,\, p,\, \alpha)\,, \quad k = 0,\, 1, \ldots,\, 2m\,.$$

These equations are solved in terms of $Y^1 = \mathbf{r}\theta$, where $\mathbf{r}$ is the right eigenvector of $G(j\omega,\, p,\, \alpha)J$ associated with the eigenvalue $\check{\lambda}$, and $\theta$ is the amplitude of the periodic solution.

The final result is obtained by computing several complex numbers, $\xi_m(\mathbf{r},\, \omega)$, which are used to graphically estimate the amplitude and frequency of the periodic solution [Moiola & Chen, 1996]. This requires solving the following equation:

$$\check{\lambda}(j\omega;\, p,\, \alpha) = -1 + \sum_{k=1}^{m} \xi_k(\mathbf{r},\, \omega)\theta^{2k}\,. \qquad (69)$$

A solution pair, $(\tilde{\omega},\, \tilde{\theta})$, is then placed in (68), so as to obtain the predicted periodic solution. For simplicity, $L_j$ is used to represent the right-hand side of Eq. (69), namely,

$$L_j = -1 + \sum_{k=1}^{j} \xi_k(\mathbf{r},\, \omega)\theta^{2k}, \quad j = 1,\, 2, \ldots,\, q\,. \qquad (70)$$

Then, under small variations in the main and auxiliary bifurcation parameters, $p$ and $\alpha$, two distinct local bifurcation phenomena, $H_{01}$ and $H_{10}$, can be found [Moiola & Chen, 1996].

To accomplish this task, it is proposed here to use a parametrized controller, $u(x;\, p,\, \alpha)$ or directly varying the system parameters (this is referred to as "parametric control") in (65), with the purpose of modifying the amplitudes or multiplicities of limit cycles near the existing Hopf bifurcation points (16). This feedback law should not modify the location of the other equilibrium points that are not related to the Hopf bifurcations. Under small variations in $p$ and $\alpha$, one can find distinct local bifurcation diagrams (i.e. plots of equilibrium and periodic solutions), in the unfoldings of $H_{01}$ and $H_{10}$ degenerate Hopf bifurcations.

First, let us define the two types of degenerate Hopf bifurcations needed:

(i) The first type, denoted by $H_{01}$ for simplicity, refers to the failure of the transversality condition in the classical Hopf bifurcation theorem, which involves the interactions of two branches of periodic solutions in its unfoldings. Then, by appropriately varying the auxiliary parameter $\alpha$ ($\alpha$, in this case, is also the unfolding parameter in the rigorous analysis of degenerate Hopf bifurcations), the two Hopf bifurcation points either gradually separate from each other, or collide together. The degeneracy exactly corresponds to the collision of the two Hopf points into a single point (middle diagrams in Fig. 17).

There are two situations to analyze, but for engineering applications it is preferable to deal with the upper case (denoted by "(a)") of Fig. 17 since it guarantees that the stable limit cycle disappears or, at least, that the stable periodic branch has a small amplitude. If the amplitude is not small enough, one can appropriately vary the parameters in order to find a smaller periodic orbit. It must be noticed that to guarantee the small amplitude of the periodic solutions, it is desirable that the absolute value of the stability index $\sigma_1$ be very large. This can be understood from the normal form point of view for generic Hopf bifurcations, since the control objective will be performed in the connecting branch of periodic solutions, where both Hopf points are generic.

The general problem (after using the center manifold theorem and reduced relevant dynamics in a two-dimensional problem) can be stated as:

$$\dot{x} = (\delta p + a(x^2 + y^2))x - (\omega + cp + b(x^2 + y^2))y\,, \qquad (71)$$

$$\dot{y} = (\omega + cp + b(x^2 + y^2))x + (\delta p + a(x^2 + y^2))y\,, \qquad (72)$$

which is expressed in polar coordinates as

$$\dot{r} = (\delta p + ar^2)r\,, \qquad (73)$$

$$\dot{\vartheta} = \omega + cp + br^2\,, \qquad (74)$$

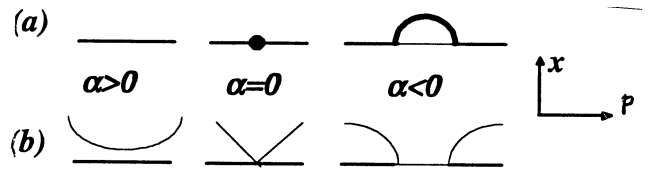


Fig. 17. Degenerate Hopf bifurcation $H_{01}$: (a) A branch of stable limit cycles, (b) A branch of unstable limit cycles.

where $\delta = \frac{d}{dp}(\Re\,\lambda_t(p)) \neq 0$, $\lambda_t$, $\bar{\lambda}_t$ are the time-domain formulas of bifurcating eigenvalues, and $a \propto \sigma_1$ is a measure of the first stability index. Then, to obtain small amplitude limit cycles for generic Hopf bifurcations, i.e. $a \neq 0$ ($\sigma_1 \neq 0$), $\delta \neq 0$, one needs to decrease the amplitude of the nonzero solution $r = \pm\sqrt{-p\delta/a}$. One way to do so is to increase the absolute value of the stability index $\sigma_1$ by using appropriate nonlinear feedback control or by parametric control.

The following algorithm has been implemented for obtaining the maximum or minimum (permissible) values of the main bifurcation control parameter and the auxiliary parameter, such that small amplitude oscillatory solutions can be sustained:

***Step 1.*** Locate an $H_{01}$-degeneracy in the parameter space ($p$, $\alpha$), and calculate the first stability index at criticality, so as to guarantee that the local bifurcation diagram has the shape of the upper diagrams (case "(a)") shown in Fig. 17. If the stability index is positive, and if there are no other eigenvalues crossing the critical point $(-1+i0)$, then the diagrams will be similar to the ones denoted as "(b)" in Fig. 17. In the latter case, another (similar) procedure, such as the one introduced in [Abed & Fu, 1986], can be applied to modify the stability of the periodic solutions, arriving at the situation depicted in Fig. 17, case "(a)".

***Step 2.*** Fix the value of the auxiliary parameter, $\alpha$, so as to have two bifurcation points after varying the bifurcation control parameter $p$. Then, solve Eq. (69) by using an iterative algorithm, introduced in [Moiola & Chen, 1996], for $q = 1, 2$, and 3.

***Step 3.*** Compare the predictions in both amplitude and frequency of different HBAs, $(\hat{\omega}_1, \hat{\theta}_1)$, $(\hat{\omega}_2, \hat{\theta}_2)$, and $(\hat{\omega}_3, \hat{\theta}_3)$, in the middle of the periodic branch. Stop the algorithm if $\max|\hat{\theta}_j - \hat{\theta}_{j+1}| > \delta_\theta$, $j = 1, 2$, where $\delta_\theta$ can be chosen as the maximum allowable difference between the two HBAs. A reasonable value for stopping would be 10 to 15% of the value of $\hat{\theta}_3$. Also, calculate the stability index $\sigma_1$ at both extremes of the local bifurcation diagram, so as to guarantee that it does not change sign. If $\sigma_1 \to 0$ at one Hopf bifurcation point, stop the algorithm at this value of $\alpha$ (since the emerging limit cycle would have a large amplitude).

***Step 4.*** Variate further the value of the auxiliary parameter, $\alpha$, in the direction along which the two bifurcation points separate from each other. Then go to Step 3.

Observe that the algorithm has a type of convergence test by itself in each evaluation by using different higher-order harmonic balance approximations (HBAs). If the three first HBAs give "coincident" results up to a certain engineering approximation, the resulting limit cycle would be of small amplitude since the approximations are local by nature. The above computations are meaningful and accurate on the basis of the existence of the $H_{01}$-degeneracy in the parameter space. This degeneracy, if not existing in the original system, can be created by an appropriate feedback control.

(ii) The second type of degenerate Hopf bifurcations, denoted $H_{10}$, concerns with the vanishing of the first stability index $\sigma_1$, or $a$ ($\propto \sigma_1$) in the Poincaré normal form of the periodic solution. This singularity produces a second limit cycle in the unfolding of the degeneracy, under a small variation of system's parameters. In other words, a nested configuration of limit cycles can be obtained, as shown in Fig. 18. Generally, the $H_{10}$-singularity has large-amplitude limit cycles emerging from criticality, and a hysteresis phenomenon. This can be used to ensure a large basin of attraction (or repulsion) for the innermost limit cycle.

It is also important to notice that one of the nondegeneracy conditions in the $H_{01}$-degeneracy is that the first stability index has a definite sign,

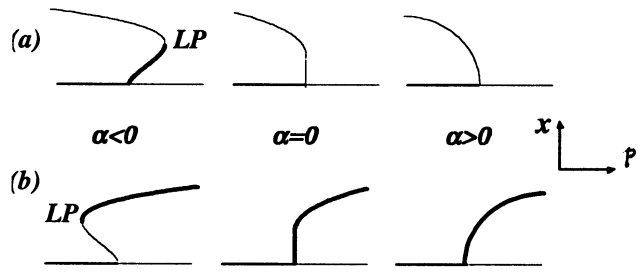


Fig. 18. Degenerate Hopf bifurcation $H_{10}$: (a) A large amplitude unstable limit cycle, (b) A large amplitude stable limit cycle. LP is a limit point (fold) of the periodic branch.

which will be maintained after the variation of the system parameters. This property can be used to control the presence of large amplitude oscillations, at least locally, in a small neighborhood of the Hopf bifurcation point.

### 7.3.2. *Controlling the amplitude of limit cycles in the electric power model*

Consider the electric power model (3). By a change of variables,

$$\theta \to x_1\,, \quad \omega \to x_2\,, \quad \theta_L \to x_3\,, \quad \text{and} \quad V_L \to x_4\,,$$

this power model is converted to the Lur'e form:

$$\begin{cases} \dot{x}(t) = Ax(t) + Bg(Cx(t);\, p,\, q) \\ y = Cx(t)\,, \end{cases}$$

where

$$A = \begin{bmatrix} -1 & 1 & 0 & 0 \\ 0 & -3.33\,q & 0 & 0 \\ 0 & 0 & -1 & -93.33 \\ 0 & 0 & 0 & -14.52 \end{bmatrix}, \quad B = C = I_4\,,$$

$$g(x(t)) := f(e(t)) = \begin{bmatrix} -e_1 \\ -16.6667\,e_4 \sin(-e_3 + e_1 + 0.0873) + 1.8807 \\ 496.8718\,e_4^2 + 166.6667\,e_4 \cos(-e_3 + e_1 - 0.0873) \\ +666.6667\,e_4 \cos(-e_3 - 0.2094) + 33.3333\,p + 43.3333 - e_3 \\ -78.763\,e_4^2 - 26.21\,e_4 \cos(-e_3 + e_1 - 0.0124) \\ -104.868\,e_4 \cos(-e_3 - 0.1346) - 29.04\,e_4 - 5.228\,p - 7.03 \end{bmatrix},$$

$$\begin{bmatrix} y_1 & y_2 & y_3 & y_4 \end{bmatrix}^\top = \begin{bmatrix} -e_1 & -e_2 & -e_3 & -e_4 \end{bmatrix}^\top,$$

and

$$G(s) = \begin{bmatrix} \dfrac{1}{s+1} & \dfrac{1}{(s+3.33\,q)(s+1)} & 0 & 0 \\ 0 & \dfrac{1}{(s+3.33\,q)} & 0 & 0 \\ 0 & 0 & \dfrac{1}{s+1} & \dfrac{-93.33}{(s+1)(s+14.52)} \\ 0 & 0 & 0 & \dfrac{1}{s+14.52} \end{bmatrix}.$$

Setting the auxiliary parameter $q = 0.109$, some local bifurcation diagrams are obtained. Two Hopf bifurcation points connected by a continuous branch of periodic solutions can be found, where the left Hopf bifurcation point has a stability index of absolute value less than that of the Hopf point on the right.

When the auxiliary parameter is gradually increased, to $q = 0.105$, larger-amplitude limit cycles are obtained in the connected branch, as shown in Fig. 19. In this figure, the predicted $\theta$ is $\hat{\theta} = 0.180267$, with a very small ($< 4\%$) relative error.

Note that the control strategy described above is based on parametric variations in the model. However, feedback control design is also possible. For this particular power system model, a nonlinear feedback controller of the form $\alpha_{c1}w^2 + \alpha_{c2}w^3$ works well. The control gains $\alpha_{c1}$ and $\alpha_{c2}$ can be tuned to enlarge the absolute value of the stability index at will. For example, amplitudes of limit cycles can be controlled to zero by a suitable choice of $\alpha_{c1}$ and $\alpha_{c2}$, in such a way that the first stability index, $\sigma_1$, does not vanish [Moiola *et al.*, 1997a; Nayfeh *et al.*, 1996; Wang & Abed, 1993].

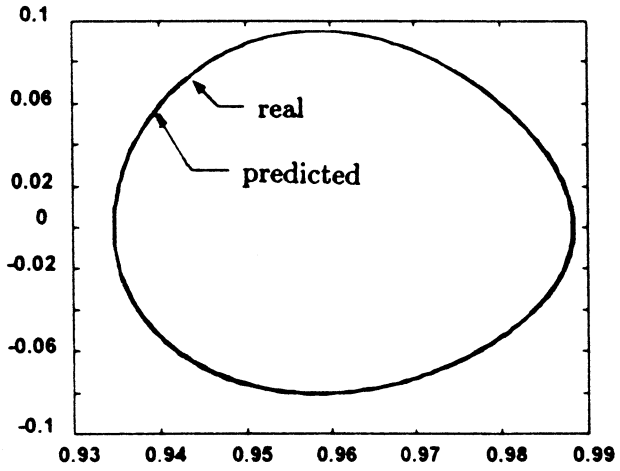


Fig. 19. Simulation results for controlling amplitudes of limit cycles in a power system.

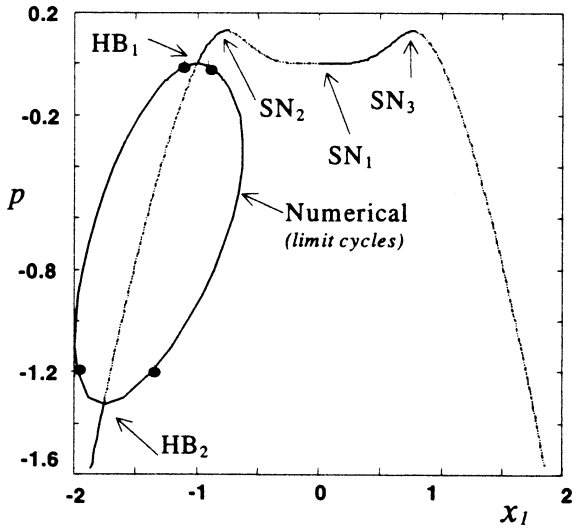


Fig. 20. Static and dynamic bifurcation varying the main bifurcation parameter $p$. The frequency domain method approximates the emerging limit cycles up to the black dots due to the large amplitude oscillations of the periodic branch.

### 7.3.3. *Controlling the amplitude and multiplicity of limit cycles in a planar system*

The above-described algorithm has been applied to controlling the amplitude of oscillations to the planar system given by Eq. (50). Notice that the results obtained by using HBAs and that obtained by numerical integrations coincide only within a small region of the main bifurcation parameter: from Hopf bifurcations up to the points marked by black-dots in Fig. 20 [Berns *et al.*, 1998a]. In order to reduce the size of the amplitudes of the oscillatory solutions located in between the two Hopf points, and then to recover the periodic solutions for a large extent of the bifurcation control parameter, the following nonlinear feedback law, $u(x;\, p,\, \alpha)$, can be added to the first equation of the system:

$$\dot{x}_1 = -x_1 x_2 + x_2^2 + p + u(x;\, p,\, \alpha)\,,$$
$$\dot{x}_2 = -x_2 + x_1^3 + p x_2\,.$$

The goal is to indirectly increase the value of $\sigma_1$, thereby decreasing the amplitudes of the limit cycles.

However, this feedback law should not modify the equilibrium points, and, if possible, should not change the location of the Hopf bifurcation points either. To fulfill these two requirements, a simple choice of the control law is

$$u(x;\, p,\, \alpha_3) = \alpha_3 \dot{x}_2^3\,, \tag{75}$$

where $\alpha_3$ is the constant control gain to be further determined. It is easy to verify, by definition, that

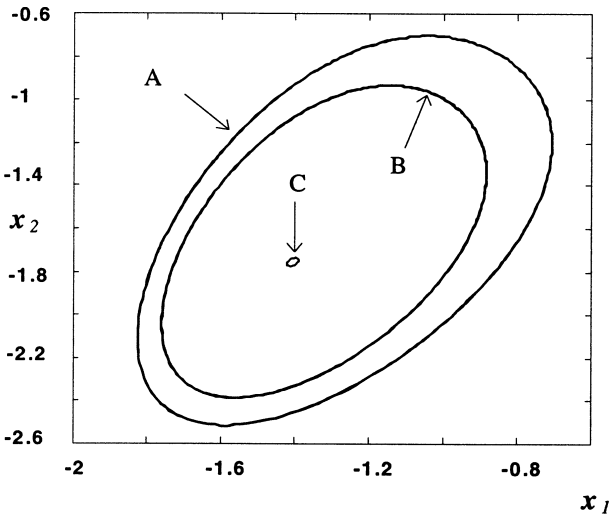


Fig. 21. Numerical solution for $p = -0.6$. "A" is a large amplitude limit cycle of the original system, and "B" and "C" are smaller limit cycles with $u = \alpha_3 \dot{x}_2^3$ ($\alpha_3 = -10$) and $u = \alpha_1 \dot{x}_2$ ($\alpha_1 = -0.01$), respectively.

the equilibrium points do not change. Moreover, neither $G(s)$ nor $J$ is modified, because the feedback law only affects the derivatives of the function $f(e)$, which has a degree equal to or greater than 3.

When $\alpha_3 = -10.0$ is used, the predicted solutions obtained using $L_1$ and $L_2$ are both difficult to be distinguished from the true limit cycle, even for the worst value of $p$, $p = -0.6$, which is in the middle of the periodic branch. To compare the reduction of the amplitudes of the limit cycles when

$p = -0.6$, Fig. 21 includes the original (without feedback) oscillatory solution (marked as "A"), and the one obtained by using the above feedback law (marked as "C"). If one only wants to preserve the equilibrium points but change the Hopf bifurcation points, then the following simpler feedback law may be used:

$$u(x;\, p,\, \alpha_1) = \alpha_1 \dot{x}_2\,. \tag{76}$$

However, it does change the location of the Hopf bifurcations points, and, by varying appropriately the value of $\alpha_1$, one can obtain the three upper local bifurcation diagrams of Fig. 17.

Figure 21 shows the largest limit cycle for the case of $p = -0.6$ with this feedback law (marked as "B"). This can be compared to the large-amplitude limit cycle of the uncontrolled system (labeled "A"), and to the one generated by the first feedback law (noted as "C"). In so doing, eventually, for a certain critical value of $\alpha_{1c}$, both HB1 and HB2 points collide into an $H_{01}$-degenerate Hopf bifurcation. In the investigation of this phenomenon, after some algebraic calculations, one obtains the location of the degenerate Hopf bifurcation point, as

$$\alpha_{1H_{01}} = -0.030979, \quad p_{H_{01}} = -0.323543\,,$$
$$(\hat{e}_1,\, \hat{e}_2) = (1.2479,\, 1.46825)\,.$$

Therefore, with the second feedback law, one has the ability to control the periodic branch (in both amplitude and frequency of the oscillations), in a way similar to handling the local bifurcation diagrams arising in the unfoldings of an $H_{01}$-degenerate Hopf bifurcation. In this control process, the constant gain $\alpha_1$ actually replaces the role of the auxiliary parameter $\alpha$ introduced before.

Next, consider changing the limit cycle multiplicity by introducing the following nonlinear law:

$$u(x;\, p,\, \alpha_1) = \alpha_2 \dot{x}_2^2 + \alpha_3 \dot{x}_2^3\,, \tag{77}$$

where $\alpha_2 = -0.17$ and $\alpha_3 = -0.015$. By computing the local bifurcation diagram with a continuation software package such as LOCBIF [Khibnik *et al.*, 1993], it ends up with a similar graph as the one to the bottom of Fig. 18, as it is shown in Fig. 22 (see [Moiola *et al.*, 1999] for more details).

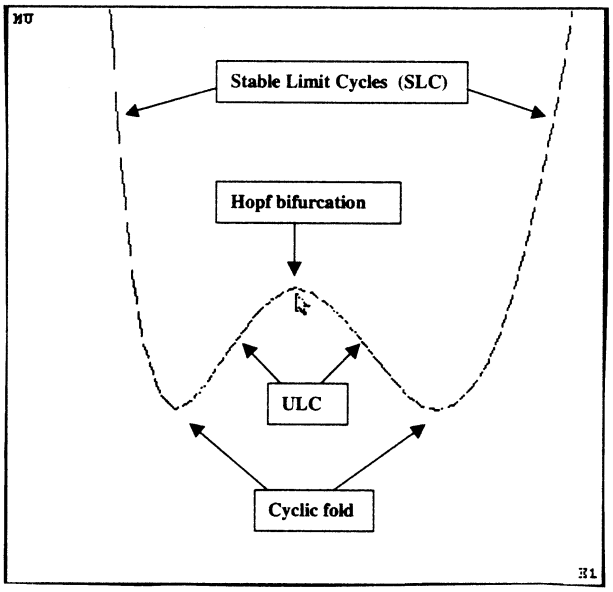


Fig. 22. Local bifurcation diagram near $H_{10}$-degeneracy. The limits of the figure are: $p_{\max} = -1.3$, $p_{\min} = -1.35$, $x_{1\,\max} = -1.5$, $x_{1\,\min} = -2$ ($\alpha_2 = -0.17$, $\alpha_3 = -0.015$).

## 8. Potential Applications of Bifurcation Control

Bifurcation control is useful in many engineering applications. Due to the vast and still rapidly growing array of information on potential applications of bifurcation control in engineering systems, it is literally impossible to give an all-rounded and comprehensive coverage of these materials in one single section of this article. Therefore, only a couple of topics that are familiar to the authors are presented here, leaving a large volume of literature to the interested reader to search.

### 8.1. *Application in cardiac alternans and rhythms control*

One interesting application of bifurcation control is the control of pathological heart rhythms [Brandt & Chen, 1997; Chen *et al.*, 1998a; Wang *et al.*, 1997, 1998]. The rhythm of the heart is determined by a wave of electrical impulses (in the form of action potential), which travels in the heart condition pathway. Arrhythmias in the heart such as fibrillation and ectopic foci are life threatening. Understanding the mechanism leading to arrhythmias is an important medical problem with enormous impact. Within this context, an even more challenging problem is the control and curing of such abnormal biological disorders. For a control engineer, a

natural question is concerning with the role of feedback in such situations. From a bifurcation control point of view, what is interesting about arrhythmias is that they have been closely linked to a variety of bifurcations, both static and dynamic, and chaos (e.g. see [Chay, 1995; Garfinket *et al.*, 1992]). This connection enables bifurcation control methods to be used for controlling heart rhythms.

As an illustration, dynamic bifurcation control is applied to suppression of pathological rhythm (cardiac alternans) in an atrioventricular modal conduction model [Sun *et al.*, 1995]. It is shown in [Sun *et al.*, 1995] that this theoretical model, which incorporates physiological concepts of recovery, facilitation and fatigue, can accurately predict a variety of experimental observed complex rhythms of nodal conduction.

Specifically, the model proposed in [Sun *et al.*, 1995] was based on stimulus-response measurements from six isolated rabbit hearts. The model is used for describing electrical conduction through the atrioventricular (AV) node, which can explain the pathological cardiac alternans. According to that reference, the atrial-His interval $A_{i+1}$, which is between cardiac impulse excitation of the low interatrial septum and the bundle of His during the $(i+1)$st cardiac cycle, is determined by the previous atrial-His interval $A_i$ and the AV nodal recovery time $H_i$:

$$\begin{aligned} A_{i+1} &= f(A_i, H_i) \\ &= A_{\min} + R_{i+1} + \beta_i \exp\left(-\frac{H_i}{\tau_{\rm rec}}\right), \end{aligned} \tag{78}$$

$$R_0 = \gamma \exp\left(-\frac{H_0}{\tau_{\rm fat}}\right), \tag{79}$$

$$\begin{aligned} R_{i+1} &= R_i \exp\left[-\frac{(A_i + H_i)}{\tau_{\rm fat}}\right] \\ &\quad + \gamma \exp\left(-\frac{H_i}{\tau_{\rm fat}}\right), \end{aligned} \tag{80}$$

$$\beta_i = \begin{cases} 201 \text{ ms} - 0.7A_i, & \text{for } A_i < 130 \text{ ms} \\ 500 \text{ ms} - 3.0A_i, & \text{for } A_i \geq 130 \text{ ms}, \end{cases} \tag{81}$$

in which $H_0$ is the initial $H$ interval and the parameters $A_{\min}$, $\tau_{\rm rec}$, $\gamma$ and $\tau_{\rm fat}$ are positive constants.

When the rabbit hearts were electrically stimulated at a fixed time period $S$ following bundle of His activation, a kind of reentrant tachycardia is observed with the $A$ intervals demonstrating an alternating time series. This can be simulated in the model by substituting the constant $S$ interval for $H_i$ with $S < 57$ ms. In the subsequent analysis, $S$ (in $H_i = S$) is used as the bifurcation parameter.

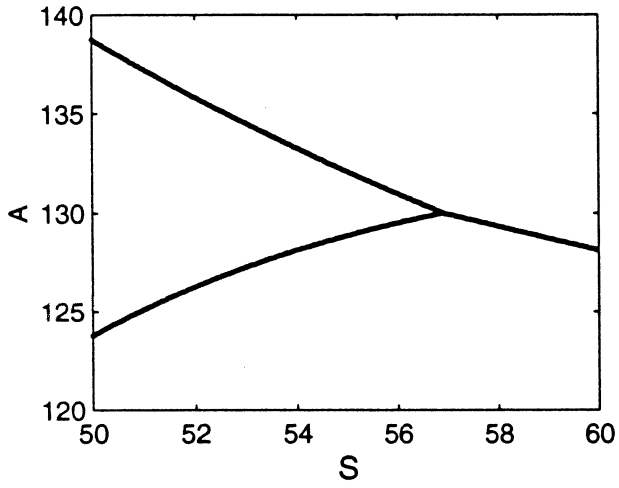


Fig. 23. Bifurcation diagram of open-loop AV nodal conduction model.

Using $S$ as the bifurcation parameter, Fig. 23 shows a bifurcation diagram of the cardiac system (78)–(81). It can be seen that there is a period-1 to period-2 bifurcation occurring near $S = 57$. Cardiac alternans arise at this bifurcation. A common view is that this period-1 to period-2 bifurcation is a period-doubling bifurcation and, therefore, alternans rhythms are associated with period-doubling bifurcations. It was shown in [Chen *et al.*, 1998a] that the cardiac system (78)–(81) undergoes a so-called *border-collision bifurcations* at this bifurcation point. The control objective of [Chen *et al.*, 1998a] is to suppress the cardiac alternans utilizing a form of dynamic bifurcation control directed at the border-collision bifurcation.

To control the cardiac alternans, a small perturbation, $u_i$, is applied to the AV node recovery interval as the control input:

$$H_i = S + u_i\,. \tag{82}$$

In [Christini & Collins, 1996; Brandt & Chen, 1997], several control schemes were suggested to stabilize the model to a period-1 rhythm. Since cardiac alternans arise at the border-collision bifurcation in the model, a dynamic bifurcation control law directed at this bifurcation is employed. This technique follows the same line of work on bifurcation control as in [Abed *et al.*, 1995; Wang & Abed, 1994].

With the dynamic feedback control law, the overall closed-loop system is given by

$$A_{i+1} = f(A_i,\, S + u_i) \tag{83}$$

$$w_{i+1} = A_i + (1-d)w_i \tag{84}$$

$$z_i = A_i - dw_i \tag{85}$$

$$u_i = g(z_i)\,. \tag{86}$$

This involves the use of a discrete-time washout filter. Here, $w_i$ is the washout filter state variable, $z_i$ is the output function, $d$ $(0 < d < 2)$ is a time constant related to the washout filter, and $g(z_i)$ is the control function to be designed.

The objective is to steer $A_i$ from the pathological period-2 orbit to a period-1 one. To achieve this, a linear controller can be designed to shift the border-collision bifurcation, effectively stabilizing the branch of unstable fixed points embedded in the region of period-2 rhythm within the uncontrolled system. The control law used is

$$u_i = g(z_i) = -k_l z_i\,, \tag{87}$$

where $k_l$ and $d$ are control design parameters.

An illuminating control result, a bifurcation diagram of the controlled map, is shown in Fig. 24. It can be seen that the border-collision bifurcation at $S_c$ is eliminated and the parameter range for the stable period-1 orbit is increased. Note that the fixed point structure is preserved in the controlled system due to the washout filter-aided design.

To illustrate the effect of the controller, a simulation result is presented in Fig. 25, where $S$ is set to be a constant (45 ms). To account for noise in real-world applications, a zero-mean Gaussian white noise sequence, $\xi_i$ ($\sigma_\xi = 1$ ms), was added to $S$, and $A_i$ was assumed to be measured with a precision of 0.5 ms, to simulate the measurement noise.

Recently, some experiments were conducted for suppressing the alternans rhythm in a piece of dissected rabbit heart [Hall *et al.*, 1997], where the control algorithm used is

$$u_i = \frac{\alpha(x_i - x_{i-1})}{2}\,. \tag{88}$$

When substituting $d = 1$ and $k_l = \alpha/2$ into (83)–(86) and (87), one can see that (88) is a special case of the linear controller (83)–(86) and (87). In [Hall *et al.*, 1997], it was shown that when using the controller (88) in the experiments, the original system's unstable period-1 equilibrium can be targeted exactly even in the case of slow evolution of the equilibria. This demonstrates the validity and robustness of the controller (83)–(86). Moreover, the bifurcation control methods proposed in [Abed *et al.*, 1995; Chen *et al.*, 1998; Wang & Abed, 1994] offer considerably flexibility in the achievable performance and dynamics of the closed-loop system.

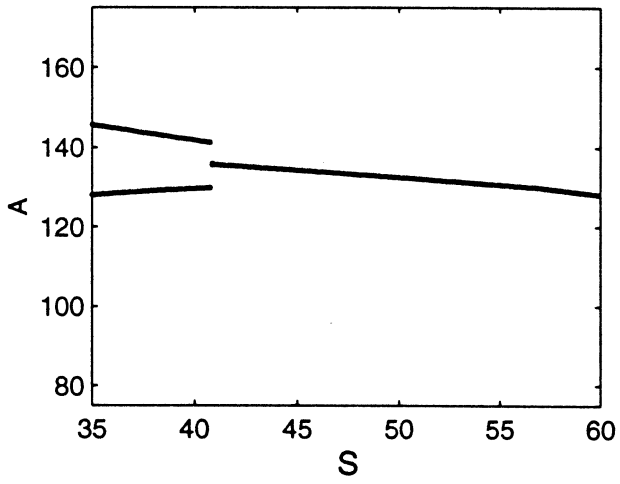


Fig. 24. Bifurcation diagram of the AV nodal conduction model under linear dynamic control: $k = 0.85$, $d = 0.1$.

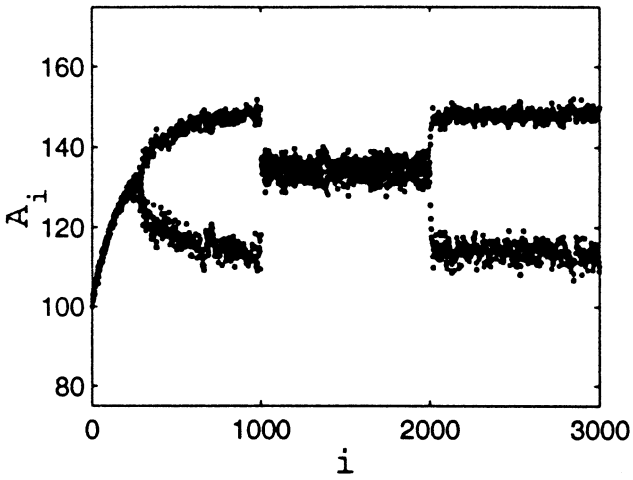


Fig. 25. Linear dynamical bifurcation control of the AV nodal conduction model with environment and measurement noise.

## 8.2. *Application in power network control and stabilization*

Nonlinearity is an inherent and essential charac-

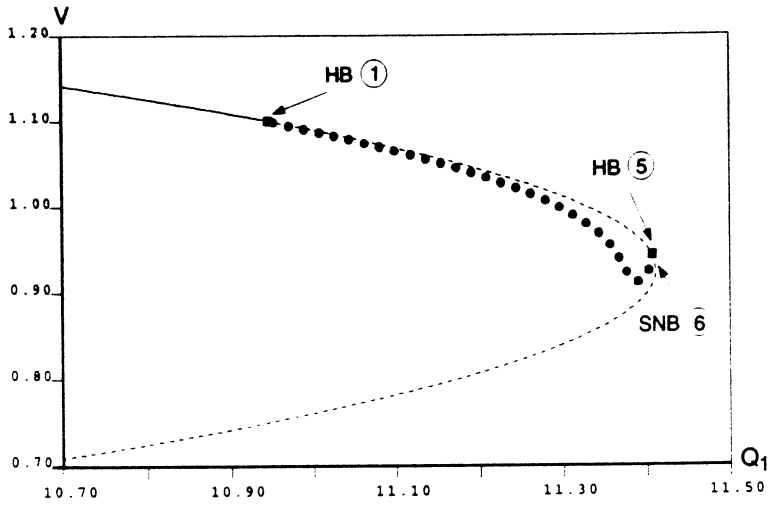


Fig. 26. Bifurcation control of voltage collapse.

teristic of electric power systems, especially in heavily loaded operation. Historically, power systems were designed and operated conservatively and, as a result, systems were normally operated within a region where system dynamical behaviors were fairly linear. Only occasionally would systems be forced to the limits where nonlinearities could begin to have significant impacts on the system behaviors.

Notably, the recent trend has different promises. Economic and environmental factors, along with the current trend towards an open access market, have strongly demanded that power systems be operated much closer to their limits as they become more heavily loaded. Ultimately, there will be greater dependence on control methods that can enable the system capability rather than on expensive physical system expansion. It is therefore vital to gain greater understanding of the nonlinear phenomena of an operational power system [Hill, 1995] and, even more significantly, the human ability to control them [Hill *et al.*, 1993].

The electric power system (3), featured in Secs. 1 and 7.3.2, was proposed in [Chiang *et al.*, 1990] as an example of exhibiting voltage collapse. Voltage collapse refers to an event in which the voltage magnitudes in AC power systems decline to some unacceptably low levels that can lead to system blackout. The power system model (3) exhibits rich nonlinear phenomena, including bifurcations and chaos. The following presents a bifurcation control approach to the problem of controlling voltage collapse [Wang & Abed, 1993] in model (3).

Consider the model (3) subject to control $u$ which is added to the right-hand side of the last equation. Note that the control occurs in the excitation system and involves a purely electrical controller. Feedback signals, which are some dynamic functions of the speed $\omega$, are widely used in power system stabilizers (PSS).

A nonlinear bifurcation control law of the form [Wang & Abed, 1993]

$$u = k_n \omega^3$$

transforms the subcritical Hopf bifurcation to a supercritical bifurcation. It also ensures a sufficient degree of stability of the bifurcated periodic solutions, so that chaos and crises are eliminated. This control law allows stable operation very close to the point of impending collapse (saddle node bifurcation). Figure 26 shows a bifurcation diagram for the closed-loop system with control gain $k_n = 0.5$.

Another linear bifurcation control law

$$u = k_l \omega$$

involves changing the critical parameter value, at which the Hopf bifurcations occur, by a linear feedback control. This linear feedback law eliminates the Hopf bifurcations and the resulting chaos and crises [Wang & Abed, 1993]. Therefore, the linearly controlled system can operate at a stable equilibrium up to the saddle node bifurcation.

In summary, although the relative importance of the effects of the nonlinear phenomena in general power systems under stressed conditions is still

a topic for further research [Hill, 1995], the bifurcation control approach appears to be a viable technique for controlling these systems.

### 8.3. *Application in axial flow compressor and jet engine control*

An application of bifurcation control is in the axial flow compressors, which are the hearts of aeroengines. Recent years have witnessed a flurry of research activities in axial flow compressor dynamics, both in terms of analysis of stall phenomena and their control. This interest is due to the increased performance that is potentially achievable in modern gas turbine jet engines by operating near the maximum pressure rise. The increased performance comes at the price of a significantly reduced stability margin. Specifically, axial flow compressors are subject to two distinct aerodynamic instabilities, rotating stall and surge, which are associated with bifurcations [McCaughan, 1989]. Both these instabilities are disruption of the normal operating condition that is designed for steady and axisymmetric flow, and both can bring catastrophic consequences to jet airplanes. Because these instabilities occur at the critical operating point of the highest pressure rise, the compressors are forced to operate at a much lower pressure rise in order to provide adequate stability margin which limit greatly the performance of axial flow compressors.

Due to the design constraint, there has been much work on enhancing compression system stability using active control. Many of the early control strategies were designed to extend the stable axisymmetric operating range by delaying the onset of stall (see, e.g. [Day, 1993; Paduano *et al.*, 1993]). The application of bifurcation control to compression system has initiated a promising paradigm aiming at solving this challenging problem [Liaw & Abed, 1992; Wang *et al.*, 1993; Badmus *et al.*, 1993]. These bifurcation control approaches look for controllers to enhance the operability of the compression system by modifying the *nonlinear* stability characteristics of the compression system. The model utilized in these studies is the so-called third-order Moore–Greitzer model [Moore & Greitzer, 1986], which is viewed as the simplest formulation that captures the physics of stall and surge phenomena. It was found that the first stalled flow solution is born through a subcritical bifurcation. The practical importance of the subcritical stall bifurcation is that when the axisymmetric flow operating point becomes subject to perturbations, the system will jump to a large-amplitude, fully developed stall cell. Subcritical bifurcations also imply hysteresis, and so returning the throttle to its original position may not bring the system out of stall.

The control strategy of [Liaw & Abed, 1992; Wang *et al.*, 1993; Badmus *et al.*, 1993] seeks to transform the hard subcritical bifurcation at the onset of stall into a soft supercritical bifurcation, thereby eliminating the hysteresis associated with rotating stall. The compressor stall application is an excellent example for illustration (both theory and experimental validation) of a guiding philosophy in bifurcation control. It relates to stabilization, or "softening," of bifurcations, with implications to improving system performance and robustness [Abed & Fu, 1986, 1987; Abed & Wang, 1995; Abed *et al.*, 1995]. Similar control strategy was utilized in [Behnken *et al.*, 1995] and a number of other research work. Others [Krstic *et al.*, 1995; Krstic *et al.*, 1998] employed more conventional control approaches such as backstepping technique to arrive at control laws for surge and rotating stall.

Some recent results on bifurcation control of compression systems involves output feedback [Gu *et al.*, 1999], which assume that the unstable modes corresponding to the critical eigenvalue of the linearized system are not linearly controllable. The first one is the stabilizability condition for the case where the critical mode is not linearly observable through output measurement. It was shown [Gu *et al.*, 1999] that nonlinear controllers do not offer any more advantage over the linear ones for bifurcation stabilization in this case. The second one is stabilizability conditions for the situation where the critical mode is linearly observable through output measurement that includes state feedback as a special case. It is shown that linear controllers are adequate for stabilization of transcritical bifurcation, and quadratic controllers are adequate for stabilization of pitchfork and Hopf bifurcations, respectively. More importantly, the stabilizability conditions are characterized in explicit forms that can be used to synthesize stabilizing controllers, if they exist.

Other work in bifurcation control include stability analysis [Gu *et al.*, 1998] and feedback stabilization [Belta *et al.*, 1999] for a partial differential equation model of the compression system. An interesting result in [Belta *et al.*, 1999] is that the proposed feedback control law requires no distributed

sensors and actuators for stabilization of the partial differential equation model described in [Moore & Greitzer, 1986].

Finally, surge control is also an interesting topic for study along this line of research [Kang *et al.*, 1999].

### 8.4. *Other examples of bifurcation control applications*

In some physical systems, such as the stressed system, delay of bifurcations offers an opportunity to obtain stable operating conditions for the machine beyond the margin of operability at the normal situation [Abed *et al.*, 1995]. Sometimes, it is desirable that the stability of bifurcated limit cycles can be modified, with application to some conventional control problems such as thermal convection experiments [Wang & Abed, 1995]. Other examples include stabilization via bifurcation control in tethered satellites [Liaw & Abed, 1990], magnetic bearing systems [Mohamed & Emad, 1993], voltage dynamics of electric power systems [Wang & Abed, 1993]; delay of bifurcation in compressor stall in gas turbine jet engines [Baillieul *et al.*, 1995; Wang *et al.*, 1993], in rotating chains via external periodic forcing [Weibel & Baillieul, 1997], and in various mechanical systems such as robotics and electronic systems such as laser machines and nonlinear circuits [Chen & Dong, 1998].

A list of potential applications of bifurcation control can be continued. The readers with interest in some specific applications of bifurcation as well as chaos control are referred to the aforementioned literature and the references therein, and particularly these very recent source books in this field, [Chen & Dong, 1998; Chen, 1999a, 1999b].

## 9. Some Concluding Remarks

This article has summarized some of the motivation, techniques and, results achieved to date on control of bifurcations. A number of representative approaches have been discussed in detail. A few remarks are in order.

The basic state feedback bifurcation control method covered in Sec. 5 deals with bifurcations in one-dimensional discrete-time and two-dimensional continuous nonlinear systems. The method is a good starting point to understand how a control input can be selected through some routine step-by-step checking procedure, so as to result in desired modifications on the system's bifurcation behaviors. In order to handle nonlinear systems of higher dimensions, however, one has to resort to alternative approaches. In this regard, the pioneering work of bifurcation control method (state feedback and/or dynamic feedback) discussed in Sec. 6.1 is directly applicable to nonlinear systems of any finite order, given in either discrete-time or continuous-time forms, not requiring invariant manifold reduction or coordinate transformation. The method in Sec. 6.1 has developed into a growing set of tools dealing with stationary bifurcations (pitchfork bifurcation, transcritical bifurcation), Hopf bifurcation and period-doubling bifurcation in general $n$-dimensional parameterized nonlinear systems. Moreover, the dynamic feedback controllers feature equilibrium preservation even in the presence of model uncertainty, and automatic targeting of the orbits to be controlled.

Normal forms are one of the powerful tools for analyzing bifurcations in nonlinear dynamical systems. Therefore, it is natural to develop normal form based control design techniques for bifurcation control problems. This method, which is presented in Sec. 6.1, applies coordinate transformations to arrive at the so-called control normal forms for nonlinear control systems. These control normal forms offer important insights into the significant role of invariants which characterize the nonlinear behavior of the system.

For continuous-time systems with limit cycles, the harmonic balance based bifurcation control discussed in Sec. 6.3 is readily applicable and efficient. The main reason is that limit cycles generally do not have analytic forms and have to be approximated in applications. Finally, to deal with Hopf bifurcation induced limit cycles as well as multiple limit cycles associated with degenerate Hopf bifurcations, the frequency domain based graphical bifurcation control method in Sec. 7, can be employed. Both amplitude and multiplicity of limit cycles can be controlled via this method.

In summary, bifurcation control involves designing a control input for a system to result in desired modification to the system's bifurcation behavior. For a given application, which approach to be employed depends largely on the nature of the problem, the familiarity of the designer, and the machinery of a particular approach with a sound engineering judgement.

## 10. To Probe Further

When leaving the idealized mathematical realm and looking around the natural world, one certainly finds a very interesting and realistic phenomenon — there is almost nothing that is linear but is not man-made out there, is it? The nonlinear nature of the real world, and of the real life, have brought up a great deal of technological challenges to scientists and engineers — the most difficult yet also most exciting complexities in dynamics, for which bifurcations, chaos, and fractals alike all get to interplay within a common ground of the mathematical as well as physical wonderland.

The field of bifurcation control is still very much in a rapidly evolving phase. This is the case not only in deeper and wider theoretical studies but also in many newly found real-world applications. It calls for further efforts and endeavors from the communities of engineering, physics, applied mathematics, and biological as well as medical sciences. New results and new publications on the subject of bifurcation control continue to appear, leaving a door widely open to every individual who has the desire and courage to pursue further in this stimulating and promising direction of new research.

## References


Abed, E. H. & Fu, J. H. [1986] "Local feedback stabilization and bifurcation control, I. Hopf bifurcation," *Syst. Cont. Lett.* **7**, 11–17.

Abed, E. H. & Fu, J. H. [1987] "Local feedback stabilization and bifurcation control, II. Stationary bifurcation," *Syst. Cont. Lett.* **8**, 467–473.

Abed, E. H., Wang, H. O., Alexander, J. C., Hamdan A. M. A. & Lee, H.-C. [1993] "Dynamic bifurcations in a power system model exhibiting voltage collapse," *Int. J. Bifurcation and Chaos* **3**, 1169–1176.

Abed, E. H., Wang, H. O. & Chen, R. C. [1994] "Stabilization of period doubling bifurcations and implications for control of chaos," *Physica* **D70**, 154–164.

Abed, E. H. [1995] "Bifurcation-theoretic issues in the control of voltage collapse," in *Proc. IMA Workshop on Systems and Control Theory for Power Systems*, eds. Chow, J. H., Kokotovic, P. V. & Thomas, R. J. (Springer, NY), pp. 1–21.

Abed, E. H. & Wang, H. O. [1995] "Feedback control of bifurcation and chaos in dynamical systems," in *Nonlinear Dynamics and Stochastic Mechanics*, eds. Kliemann, W. & Sri Namachchivaya, N. (CRC Press, Boca Raton, FL), pp. 153–173.

Abed, E. H., Wang, H. O. & Tesi, A. [1995] "Control of bifurcation and chaos," in *The Control Handbook*, ed. Levine, W. S. (CRC Press, Baco Raton), FL, pp. 951–966.

Alhumaizi, K. & Elnashaie, S. E. H. [1997] "Effect of control loop configuration on the bifurcation behavior and gasoline yield of industrial fluid catalytic cracking (FCC) units," *Math. Comp. Modelling* **25**, 37–56.

Alvarez, J. & Curiel, L. E. [1997] "Bifurcations and chaos in a linear control system with saturated input," *Int. J. Bifurcation and Chaos* **7**, 1811–1822.

Ananthkrishnan, N. & Sudhakar, K. [1996] "Characterization of periodic motions in aircraft lateral dynamics," *J. Guidance Contr. Dyn.* **19**, 680–685.

Argyris, J., Faust, G. & Haase, M. [1994] *An Exploration of Chaos* (North-Holland, NY).

Arrowsmith, D. K. & Place, C. M. [1990] *An Introduction to Dynamical Systems* (Cambridge University Press, NY).

Badmus, O. O., Chowdhury, S., Eveker, K. M., Nett, C. N. & Rivera, C. J. [1993] "A simplied approach for control of rotating stall, Part 2: Experimental results," Paper No. AIAA-93-2234, *29th Joint Propulsion Conference and Exhibit*, Monterey, CA.

Baillieul, J., Dahlgren, S. & Lehman, B. [1995] "Nonlinear control design for systems with bifurcations with applications to stabilization and control of compressors," *Proc. IEEE Conf. Decision Control*, pp. 3063–3067.

Basso, M., Evangelisti, A., Genesio, R. & Tesi, A. [1998] "On bifurcation control in time delay feedback systems," *Int. J. Bifurcation and Chaos* **8**, 713–721.

Behnken, R. L., D'Andrea, R. & Murray, R. M. [1995] "Control of rotating stall in a low-speed axial flow compressor using pulsed air injection: Modeling, simulations and experimental validation," *Proc. IEEE Conf. Decision and Control*, New Orleans, LA.

Belta, C., Gu, G., Sparks, A. & Banda, S. [1999] "Rotating stall and surge control for axial flow compressors," *Proc. IFAC'99*, Beijing, China.

Berns, D. W. & Moiola, J. L. [1998] "Multiple oscillations in a chemical reactor," *Latin American Appl. Res.* **28**, 49–56.

Berns, D. W., Moiola, J. L. & Chen, G. [1998a] "Feedback control of limit cycle amplitudes from a frequency domain approach," *Automatica* **34**, 1567–1573.

Berns, D. W., Moiola, J. L. & Chen, G. [1998b] "Predicting period-doubling bifurcations and multiple oscillations in nonlinear time-delayed feedback systems," *IEEE Trans. Circuits Syst. I* **45**, 759–763.

Brandt, M. E. & Chen, G. [1997] "Bifurcation control of two nonlinear models of cardiac activity," *IEEE Trans. Circuits Syst. I* **44**, 1031–1034.

Calandrini, G., Paolini, E., Moiola, J. L. & Chen, G. [1999] "Controlling limit cycles and bifurcations," in

*Controlling Chaos and Bifurcations in Engineering Systems*, ed. Chen, G. (CRC Press), pp. 200–227.

Cam, U. & Kuntman, H. [1998] "A new CCII-based sinusoidal oscillator providing fully independent control of oscillation condition and frequency," *Microelectron. J.* **29**, 913–919.

Chan, W. C. Y. & Tse, C. K. [1996] "Bifurcation in bifurcation from a current-programmed DC/DC boost converter," *Proc. IEEE Int'l Symp. Circ. Syst.*, Atlanta, GA, pp. 249–252.

Chang, F. J., Twu, S. H. & Chang, S. [1993] "Global bifurcation and chaos from automatic gain control loops," *IEEE Trans. Circuits Syst.* **40**, 403–411.

Chapman, G. T., Yates, L. A. & Szady, M. J. [1992] "Atmospheric flight dynamics and chaos: Some issues in modeling and dimensionality," in *Applied Chaos*, eds. Kim, J. H. & Stringer, J. (Wiley, NY), pp. 87–141.

Chay, T. R. [1995] "Bifurcations in heart rhythms," *Int. J. Bifurcation and Chaos* **5**, 1439–1486.

Chen, D., Wang, H. O. & Chin, W. [1998a] "Suppression cardiac alternans: Analysis and control of a border-collision bifurcation in a cardiac conduction model," *Proc. IEEE Int. Symp. Circ. Syst.*, Monterey, CA, III 635–III 638.

Chen, D., Wang, H. O. & Chen, G. [1998b] "Anti-control of Hopf bifurcations through washout filters," *Proc. 37th IEEE Conf. Decision and Control*, Tampa, FL, Dec. 16–18, 1998, pp. 3040–3045.

Chen, G. [1998] "Chaos: Control and anti-control," *IEEE Circuits and Systems Society Newsletter*, March 1998, pp. 1–5.

Chen, G. [1999a] "Chaos, bifurcation, and their control," in *The Wiley Encyclopedia of Electrical and Electronics Engineering*, ed. Webster, J. (Wiley, NY), **3**, pp. 194–218.

Chen, G. (ed.) [1999b] *Controlling Chaos and Bifurcations in Engineering Systems* (CRC Press, Boca Raton, FL).

Chen, G. & Dong, X. [1998] *From Chaos to Order: Methodologies, Perspectives and Applications* (World Scientific, Singapore).

Chen, G., Fang, J.-Q., Hong, Y. & Qin, H. [1999a] "Controlling Hopf bifurcations: The continuous case," *ACTA Physica China* **8**, 416–422.

Chen, G., Fang, J.-Q., Hong, Y. & Qin, H. [1999b] "Controlling Hopf bifurcations: The discrete case," *Dis. Dyn. Nat. Soc.*, 2000, in press.

Chen, G., Lu, J., Nicholas, B. & Ranganathan, S. M. [1999c] "Bifurcation dynamics in discrete-time delayed-feedback control systems," *Int. J. Bifurcation and Chaos* **9**, 287–293.

Chen, G., Lu, J. & Yap, K. C. [1998] "Controlling Hopf bifurcations," *Proc. Int. Symp. Circuits Systems*, monterey, CA, pp. III, 639–642.

Chen, G. & Moiola, J. L. [1994] "An overview of bifurcation, chaos, and nonlinear dynamics in control systems," *J. Franklin Institute* **331B**, 819–858.

Chen, X., Gu, G., Martin, P. & Zhou, K. [1998] "Bifurcation control with output feedback and its applications to rotating stall control," *Automatica* **34**, 437–443.

Cheng, H. [1990] "Bifurcation and stability of constrained rotational mechanical systems," in *Flexible Mechanism, Dynamics, and Robot Trajectories*, eds. Derby, S., McCarthy, M. & Pisano, A. (ASME, NY), pp. 169–176.

Chiang, H.-D., Dobson, I., Thomas, R. J., Thorp, J. S. & Fekih-Ahmed, L. [1990] "On voltage collapse in electric power systems," *IEEE Trans. Power Syst.* **5**, 601–611.

Chiang, H.-D., Conneen, T. P. & Flueck, A. J. [1994] "Bifurcations and chaos in electric power systems: Numerical studies," *J. Franklin Inst.* **331B**, 1001–1036.

Christini, D. J. & Collins, J. J. [1996] "Using chaos control and tracking to suppress a pathological nonchaotic rhythm in a cardiac model," *Phys. Rev.* **E53**, R49.

Chua, L. O. [1998] *CNN*: *A Paradigm for Complexity* (World Scientific, Singapore).

Cui, F., Chew, C. H., Xu, J. & Cai, Y. [1997] "Bifurcation and chaos in the Duffing oscillator with a PID controller," *Nonlin. Dynam.* **12**, 251–262.

Day, I. J. [1993] "Active suppression of rotating stall and surge in axial compressors," *ASME J. Turbomachinery* **115**, 40–47.

Dobson, I. & Lu, L. M. [1992] "Computing an optimum direction in control space to avoid saddle node bifurcation and voltage collapse in electric power systems," *IEEE Trans. Auto. Contr.* **37**, 1616-1620.

Dobson, I., Glavitsch, H., Liu, C. C., Tamura, Y. & Vu, K. [1992] "Voltage collapse in power systems," *IEEE Circuits and Devices Magazine* **8**, 40–45.

Garfinkel, A., Spano, M. L., Ditto, W. L. & Weiss, J. N. *et al.* [1992] "Controlling cardiac chaos," *Science* **257**, 1230–1235.

Genesio, R., Tesi, A., Wang, H. O. & Abed, E. H. [1993] "Control of period doubling bifurcations using harmonic balance," *Proc. Conf. Decis. Contr.*, San Antonio, TX, pp. 492–497.

Gibson, L. P., Nichols, N. K. & Littleboy, D. M. [1998] "Bifurcation analysis of eigenstructure assignment control in a simple nonlinear aircraft model," *J. Guidance, Contr. Dyn.* **21**, 792–798.

Glendinning, P. [1994] *Stability, Instability and Chaos* (Cambridge Univ Press, NY).

Golden, G. C. & Ydstie, B. E. [1988] "Bifurcation in model reference adaptive control systems," *Syst. Cont. Lett.* **11**, 413–430.

Golden, M. P. & Ydstie, B. E. [1992] "Small amplitude chaos and ergodicity in adaptive control," *Automatica* **28**, 11–25.

Goman, M. G. & Khramtsovsky, A. V. [1998] "Applica-

tion of continuation and bifurcation methods to the design of control systems," *Phil. Trans. R. Soc. Lond.* **A356**, 2277–2295.

Gu, G., Sparks, A. G. & Banda, S. S. [1997] "Bifurcation based nonlinear feedback control for rotating stall in axial flow compressors," *Int. J. Cont.* **6**, 1241–1257.

Gu, G., Sparks, A. G. & Belta, C. [1998] "Stability analysis for rotating stall and surge in axial flow compressors," *Proc. IEEE Conf. Dec. and Contr.*, pp. 2557–2562.

Gu, G., Chen, X., Sparks, A. G. & Banda, S. S. [1999] "Bifurcation stabilization with local output feedback," *SIAM J. Contr. Optim.* **37**, 934–956.

Hackl, K., Yang, C. Y. & Cheng, A. H. D. [1993] "Stability, bifurcation and chaos of non-linear structures with control. Part 1. Autonomous case," *Int. J. Nonlin. Mech.* **28**, 441–454.

Hale, J. & Koçak, H. [1991] *Dynamics and Bifurcations* (Springer-Verlag, NY).

Hall, K., Christini, D. J., Tremblay, M. & Collins, J. J. *et al.* [1997] "Dynamic control of cardiac alternans," *Phys. Rev. Lett.* **78**, 4518–4521.

Hassard, B. & Jiang, K. [1992] "Unfolding a point of degenerate Hopf bifurcation in an enzyme-catalyzed reaction model," *SIAM J. Math. Anal.* **23**, 1291–1304.

Hassard, B. & Jiang, K. [1993] "Degenerate Hopf bifurcation an isolas of periodic solutions in an enzyme-catalyzed reaction model," *J. Math. Anal. Appl.* **177**, 170–189.

Hill, D. J., Hiskens, I. A. & Wang, Y. [1993] "Robust, adaptive or nonlinear control for modern power systems," *Proc. 32nd IEEE Conf. Decision and Control*, San Antonio, TX, pp. 2335–2340.

Hill, D. J. (ed.) [1995] Special Issue on Nonlinear Phenomena in Power Systems, *Proc. IEEE* **83**, No. 11.

Hu, G. & Haken, H. [1990] "Potential of the Fokker–Planck equation at degenerate Hopf bifurcation points," *Phys. Rev.* **A41**, 2231–2234.

Iida, S. K., Ogawara, K. & Furusawa, S. [1996] "A study on bifurcation control using pattern recognition of thermal convection," *JSME Int. J. Series B — Fluid and Thermal Eng.* **39**, 762–767.

Invernizzi, S. & Treu, G. [1991] "Quantitative analysis of the Hopf bifurcation in the Goodwin $n$-dimensional metabolic control system," *J. Math. Biol.* **29**, 733–742.

Ji, W. & Venkatasubramanian, V. [1995] "Dynamics of a minimal power system: Invariant tori and quasi-periodic motions," *IEEE Trans. Circuits Syst.* **42**, 981–1000.

Kang, W. & Krener, A. J. [1992] "Extended quadratic controller normal form and dynamic feedback linearization of nonlinear systems," *SIAM J. Contr. Optim.* **30**, 1319–1337.

Kang, W. [1998a] "Bifurcation and normal form of nonlinear control systems," Parts I and II, *SIAM J. Contr. Optim.* **36**, 193–232.

Kang, W. [1998b] "Bifurcation control via state feedback for systems with a single uncontrollable mode," *SIAM J. Contr. Optim.*, 2000, to appear.

Kang, W., Gu, G., Sparks, A. & Banda, S. [1999] "Bifurcation test functions and surge control for axial flow compressors," *Automatica* **35**, 229–239.

Kelly, R. [1996] "Bifurcation in PD feedback regulation of a single pendulum," *Proc. 7th Congreso Latinoamericano de Control Automatico — IFAC*, Buenos Aires, Argentina, pp. 1034–1039.

Khibnik, A. I., Kuznetsov, Yu. A., Levitin, V. V. & Nikolaev, E. V. [1993] "Continuation techniques and interactive software for bifurcation analysis of ODE's and iterated maps," *Physica* **D62**, 360–371.

Krstic, M., Protz, J. M., Paduano, J. D. & Kokotovic, P. V. [1995] "Backstepping designs for jet engine stall and surge control," *Proc. 34th IEEE Conf. Decision and Control*, pp. 3049–3055.

Krstic, M., Fontaine, D., Kokotovic P. V. & Paduano, J. D. [1998] "Useful nonlinearities and global stabilization of bifurcations in a model of jet engine surge and stall," *IEEE Trans. Auto. Contr.* **43**, 1739–1745.

Laufenberg, M. J., Pai, M. A. & Padiyar, K. R. [1997] "Hopf bifurcation control in power systems with static var compensator," *Int. J. Elect. Power & Energy Syst.* **19**, 339–347.

Lee, B. & Ajjarapu, V. [1993] "Period-doubling route to chaos in an electrical power system," *IEE Proc.* Part C **140**, pp. 490–496.

Lee, H.-C. & Abed, E. H. [1991] "Washout filters in the bifurcation control of high alpha flight dynamics," *Proc. Ame. Control Conf.*, Boston, pp. 206–211.

Liaw, C. Y. & Bishop, S. R. [1995] "Nonlinear heave-roll coupling and ship rolling," *Nonlin. Dyn.* **8**, 197–211.

Liaw, D. C. & Abed, E. H. [1990] "Stabilization of tethered satellites during station keeping," *IEEE Trans. Auto. Cont.* **35**, 1186–1196.

Liaw, D. C. & Abed, E. H. [1992] "Analysis and control of rotating stall," *Proc. NOLCOS'92: Nonlinear Control System Design Symp. — IFAC*, Bordeaux, France, pp. 88–93.

Liaw, D. C. & Abed, E. H. [1996] "Control of compressor stall inception — A bifurcation-theoretic approach," *Automatica* **32**, 109–115.

Littleboy, D. M. & Smith, P. R. [1998] "Using bifurcation methods to aid nonlinear dynamic inversion control law design," *J. Guidance Contr. Dyn.* **21**, 632–638.

Liu, Z., Payre, G. & Bourassa, P. [1996] "Nonlinear oscillations and chaotic motions in a road vehicle system with driver steering control," *Nonlin. Dyn.* **9**, 281–304.

Madan, R. (ed.) [1993] *Chua's Circuit: A Paradigm for Chaos* (World Scientific, Singapore).

Malmgren, B. A., Winter, A. & Chen, D. L. [1998] "El Niño southern oscillation and north Atlantic oscillation control of climate in Puerto Rico," *J. Climate* **11**, 2713–2717.

Mareels, I. M. Y. & Bitmead, R. R. [1986] "Nonlinear dynamics in adaptive control: Chaotic and periodic stabilization," *Automatica* **22**, 641–665.

Mareels, I. M. Y. & Bitmead, R. R. [1988] "Nonlinear dynamics in adaptive control: Periodic and chaotic stabilization II — analysis," *Automatica* **24**, 485–497.

Matsumoto, T. [1987] "Chaos in electronic circuits," *Proc. IEEE* **75**, 1033–1057.

McCaughan, F. E. [1989] "Application of bifurcation theory to axial flow compressor instability," *ASME J. Turbomachinery* **111**, 426–433.

Mees, A. I. & Chua, L. O. [1979] "The Hopf bifurcation theorem and its applications to nonlinear oscillations in circuits and systems," *IEEE Trans. Circuits Syst.* **26**, 235–254.

Mohamed, A. M. & Emad, F. P. [1993] "Nonlinear oscillations in magnetic bearing systems," *IEEE Trans. Auto. Cont.* **38**, 1242–1245.

Moiola, J. L., Desages, A. C. & Romagnoli, J. A. [1991] "Degenerate Hopf bifurcations via feedback system theory — Higher-order harmonic balance," *Chem. Eng. Sci.* **46**, 1475–1490.

Moiola, J. L. & Chen, G. [1996] *Hopf Bifurcation Analysis: A Frequency Domain Approach* (World Scientific, Singapore).

Moiola, J. L., Berns, D. W. & Chen, G. [1997a] "Feedback control of limit cycle amplitudes," *Proc. IEEE Conf. Decis. Contr.*, San Diego, CA, pp. 1479–1485.

Moiola, J. L., Colantonio, M. C. & Doñate, P. D. [1997b] "Analysis of static and dynamic bifurcations from a feedback systems perspective," *Dyn. Stab. Syst.* **12**, 293–317.

Moiola, J. L. & Chen, G. [1998] "Controlling the multiplicity of limit cycles," *Proc. IEEE Conf. Decis. Contr.*, FL, pp. 3052–3057.

Moiola, J. L., Berns, D. W. & Chen, G. [1999] "Controlling degenerate Hopf bifurcations," *Latin American Appl. Res.* **29**, 213–220.

Moore, F. K. & Greitzer, E. M. [1986] "A theory of post-stall transients in axial compressors: Part I–development of the equations," *ASME J. Engr. Gas Turbines and Power* **108**, 68–76.

Moroz, I. M., Baigent, S. A., Clayton, F. M. & Lever, K. V. [1992] "Bifurcation analysis of the control of an adaptive equalizer," *Proc. R. Soc. London Series A-Math. & Phys. Sciences* **537**, 501–515.

Nayfeh, A. H., Harb, A. M. & Chin, C. M. [1996] "Bifurcations in a power system model," *Int. J. Bifurcation and Chaos* **6**, 497–512.

Ono, E., Hosoe S., Tuan H. D. & Doi, S. [1998] "Bifurcation in vehicle dynamics and robust front wheel steering control," *IEEE Trans. Contr. Syst. Technol.* **6**, 412–420.

Paduano, J. D., Epstein, A. H., Valavani, L., Longley, J. P., Greitzer, E. M. & Guenette, G. R. [1993] "Active control of rotating stall in a low-speed axial compressor," *J. Turbomachinery* **115**, 48–56.

Pinsky, M. A. & Essary, B. [1994] "Analysis and control of bifurcation phenomena in aircraft flight," *J. Guidance Contr. Dyn.* **17**, 591–598.

Praly, L. & Pomet, J. B. [1987] "Periodic solutions in adaptive systems: The regular case," *Proc. IFAC 10th Triennual World Congress* **10**, Munich, pp. 40–44.

Richards, G. A., Yip, M. J., Robey, E. & Cowell *et al.*, [1997] "Combustion oscillation control by cyclic fuel injection," *J. Eng. Gas Turbines and Power Electronics* **10**, 340–343.

Reznik, D. & Scholl, E. [1993] "Oscillation modes, transient chaos and its control in modulation-doped semiconductor double-heterostructure," *Zeitschrift für Physik B-Condensed Matter* **91**, 309–316.

Sanchez, N. E. & Nayfeh, A. H. [1979] "Nonlinear rolling motions of ships in longitudinal waves," *Shipbuilding Progress* **37**, 247–272.

Senjyu, T. & Uezato, K. [1995] "Stability analysis and suppression control of rotor oscillation for stepping motors by Lyapunov direct method," *IEEE Trans. Power Electron.* **10**, 333–339.

Shiau, L. J. & Hassard, B. [1991] "Degenerate Hopf bifurcation and isolated periodic solutions of the Hodgkin–Huxley model with varying sodium ion concentration," *J. Theoret. Biol.* **148**, 157–173.

Srivastava, K. N. & Srivastava, S. C. [1995] "Application of Hopf bifurcation theory for determining critical value of a generator control or load parameter," *Int. J. Electrical Power Energy Syst.* **17**, 347–354.

Streit, D. A., Krousgrill, C. M. & Bajaj, A. K. [1988] "Combination parametric resonance leading to periodic and chaotic response in two-degree-of-freedom systems with quadratic nonlinearities," *J. Sound Vib.* **124**, 470–480.

Sun, J., Amellal, F., Glass, L. & Billette, J. [1995] "Alternans and period-doubling bifurcations in atrioventricular nodal conduction," *J. Theor. Biol.* **173**, 79–91.

Tan, C.-W., Varghese, M., Varaiya, P. & Wu, F. F. [1995] "Bifurcation, chaos, and voltage collapse in power systems," *Proc. IEEE* **83**, 1484–1496.

Tesi, A., Abed, E. H., Genesio, R. & Wang, H. O. [1996] "Harmonic balance analysis of period-doubling bifurcations with implications for control of nonlinear dynamics," *Automatica* **32**, 1255–1271.

Thomsen, J. J. [1995] "Chaotic dynamics of the partially follower-loaded elastic double pendulum," *J. Sound Vibr.* **188**, 385–405.

Tse, C. K. [1994] "Flip bifurcation and chaos in

three-state boost switching regulators," *IEEE Trans. Circuits Syst.* **41**, 16–23.

Ueta, T., Kawakami, H. & Morita, I. [1995] "A study of the pendulum equation with a periodic impulse force — bifurcation and chaos," *IEICE Trans. Fundam. Electr. Commun. Comput. Sci.* **E78A**, 1269–1275.

Vakakis, A. F., Burdick, J. W. & Caughey, T. K. [1991] "An 'interesting' strange attractor in the dynamics of a hopping robot," *Int. J. Robot Res.* **10**, 606–618.

Venkatasubramanian, V. & Ji, W. [1999] "Coexistence of four different attractors in a fundamental power system model," *IEEE Trans. Circuits Syst. I* **46**, 405–409.

Volkov, A. N. & Zagashvili, U. V. [1997] "A method of synthesis for automatic control systems with maximum degree of stability and given oscillation index," *J. Comput. Systs. Sci. Int.* **36**, 29–34.

Wang, H. O. & Abed, E. H. [1993] "Control of nonlinear phenomena at the inception of voltage collapse," *Proc. Am. Contr. Conf.*, San Francisco, CA, pp. 2071–2075.

Wang, H. O., Adomaitis, R. A. & Abed, E. H. [1993] "Active stabilization of rotating stall in axial-flow gas compressors," *Proc. IEEE Conf. Aero. Contr. Syst.*, Westlake Village, CA, pp. 498–502.

Wang, H. O. & Abed, E. H. [1994] "Robust control of period doubling bifurcations and implications for control of chaos," *Proc. 33rd IEEE Conf. Decision and Control*, Orlando, pp. 3287–3292.

Wang, H. O., Abed, E. H. & Hamdan, M. A. [1994a] "Bifurcations, chaos, and crises in voltage collapse of a model power system," *IEEE Trans. Circuits Syst.* **41**, 294–302.

Wang, H. O., Adomaitis, R. A. & Abed, E. H. [1994b] "Active control of rotating stall in axial-flow compressors," *Proc. 1994 Am. Control Conf.*, Baltimore, MD, pp. 2317–2321.

Wang, H. O. & Abed, E. H. [1995] "Bifurcation control of a chaotic system," *Automatica* **31**, pp. 1213–1226.

Wang, H. O., Chen, D. & Bushnell, L. G. [1997] "Control of bifurcations and chaos in heart rhythms," *Proc. 36th IEEE Conf. Decision Control*, San Diego, CA, pp. 395–400.

Wang, H. O., Chen, D. & Chen, G. [1998] "Bifurcation control of pathological heart rhythms," *Proc. IEEE Conf. Contr. Appl.*, Trieste, Italy, pp. 858–862.

Weibel, S. & Baillieul, J. [1997] "Oscillatory control of bifurcations in rotating chains," *Proc. Amer. Contr. Conf.*, Albuquerque, NM, 2713–2718.

Wiggins, S. [1988] *Global Bifurcations and Chaos* (Springer-Verlag, NY).

Wiggins, S. [1990] *Introduction to Applied Nonlinear Dynamical Systems and Chaos* (Springer-Verlag, NY).

Yabuno, H. [1997] "Bifurcation control of parametrically excited Duffing system by a combined linear-plus-nonlinear feedback control," *Nonlin. Dyn.* **12**, 263–274.

Yap, K. C. & Chen, G. [2000] "Controlling bifurcations of discrete maps," preprint.

Ydstie, B. E. & Golden, G. C. [1986] "Bifurcation and complex dynamics in adaptive control systems," *Proc. IEEE Conf. Decision Contr*, Athens, pp. 2232–2236.

Ydstie, B. E. & Golden, M. P. [1987] "Chaos and strange attractors in adaptive control systems," *Proc. IFAC World Congress* **10**, Munich, pp. 127–132.

Ydstie, B. E. & Golden, M. P. [1988] "Chaotic dynamics in adaptive systems," *Proc. IFAC Workshop on Robust Adaptive Control*, Newcastle, pp. 14–19.

Zhou, F. & Nossek, J. A. [1993] "Bifurcation and chaos in cellular neural networks," *IEEE Trans. Circ. Syst. I* **40**, 843–848.

Zhou, Z. & Whiteman, C. [1996] "Motions of a double pendulum," *Nonlin. Anal. Th. Meth. Appl.* **26**, 1177–1191.